

# Ocean mixed layer response to the tropical cyclone moving in different directions in the south Indian Ocean

A.A.Deo, D.W.Ganer and P.S.Salvekar  
Indian Institute of Tropical Meteorology, Pune 411 008  
E-mail : [aad@tropmet.res.in](mailto:aad@tropmet.res.in)

## Introduction

For the dynamical prediction of tropical cyclone the knowledge about the ocean response to storm forcing is essential. In the earlier studies the surface circulation and mixed layer depth variation in response to moving cyclones in the Indian Ocean has been studied considering idealized vortex and tracks by using 1½ layer reduced gravity ocean model.<sup>2,3,4,5</sup> In the present study the thermodynamics is included to study the variation in the temperature of the mixed layer during the passage of the cyclone. The model circulation, mixed layer depth variation and temperature change are compared for two different tracks in the southern hemisphere.

## Numerical experiment

The 1½ layer reduced gravity ocean model<sup>1</sup> is now modified by including thermodynamic equation which contains the advection term, horizontal diffusion term and the effect of vertical mixing with bottom water. The cooling by evaporation and the effect of sensible heat transfer are neglected as in earlier study<sup>3</sup>. The effect of vertical mixing terms is incorporated implicitly, so that the final temperature equation uses the mixed layer depth before and after entrainment as well as the temperature difference between the mixed layer and the bottom layer. The initial thermocline is assumed to be 50 m deep with top and bottom layer temperatures as 29C and 22C respectively.

Two cases of storm tracks in the southern hemisphere have been chosen. The idealized symmetric cyclonic vortex (Similar to Rankine vortex) having radius 400 km and maximum winds 20 m/s is allowed to move on two tracks say, Track 1 and Track 2. Track 1 is westward, along the line joining the points (70E,15S) and (61E,15S) and Track 2 is southward, along the line joining the points (90E,5S) and (90E,14S). These tracks are close to the observed tracks of the cyclones Mariola (21 S) and Willy (30S) of the year 1994. The duration of the storm in both the cases is kept 5 days so that the storm speed remains same and hence the model integration is carried out for 5 days.

## Results and conclusion

Figure 1 shows the model currents, upper layer thickness deviation (ULTD) and temperature change on fourth day for Track 1 (left panel) and for Track 2 (right panel). Results indicate that the maximum currents, ULTD and temperature change has left bias for Track 2 and no bias for Track 1, which are in agreement with earlier reported work<sup>4,5</sup>. However for Track 1, the region of cooling tilts to the left side of the track which suggests that the mixed layer on the left, is cooled slightly more than the right of both the tracks for all the tracks. The number of waves in the ULTD field are in correspondence with the number of waves in temperature field. The area of temperature change is widely spread as compared to that of upper layer thickness deviation. Consequently, the lag between the storm position and maximum cooling is less than that of maximum upwelling. The inertial wave in the wake of the cyclone is clearly seen for Track 1 but is not seen for Track 2. The maximum magnitude of currents (.4 m/s), upwelling (10 m) and cooling (2 C) is less for Track 1 as compared to that for Track 2 for which these values are .6 m/s, 20m and 4 C. These results are found to be reversed in the northern hemispheric cases of cyclones the in earlier study<sup>4</sup>, where it was found that the magnitude of maximum upwelling is significantly less for the northward track than that for the westward track. From this study it can be said that the results of both the hemisphere differ mainly because of the sign of coriolis parameter.

## References

1. Behera S.K and Salvekar P.S, 1996: Development of simple reduced gravity ocean model for the study of upper north Indian Ocean. S.K, I.I.T.M. Reaserch Report, pp 36.
2. Behera S.K, Deo A.A, and Salvekar P.S., 1998: Investigation of mixed layer response to Bay of Bengal cyclone using a simple ocean model. Meteorol. Atmos. Phys.,65, 77-91.
3. Chang S.W. & Anthes R.A., 1978: Numerical simulation of the ocean's nonlinear baroclinic response to translating hurricanes. J. Phys. Oceano., 13, 468-480
4. Deo A.A, Salvekar P.S and Behera S.K,2001a: Oceanic response to cyclone moving in different directions over Indian Seas using IRG model. Mausam, 52, 163-174.
5. Deo A.A,Ganer, D.W.,& Salvekar P.S,2001b: Upper ocean response to a moving cyclone in south Indian Ocean. WGNE Report on Research Activities in Atmospheric and Ocean Modelling,, pp 8.3-8.4

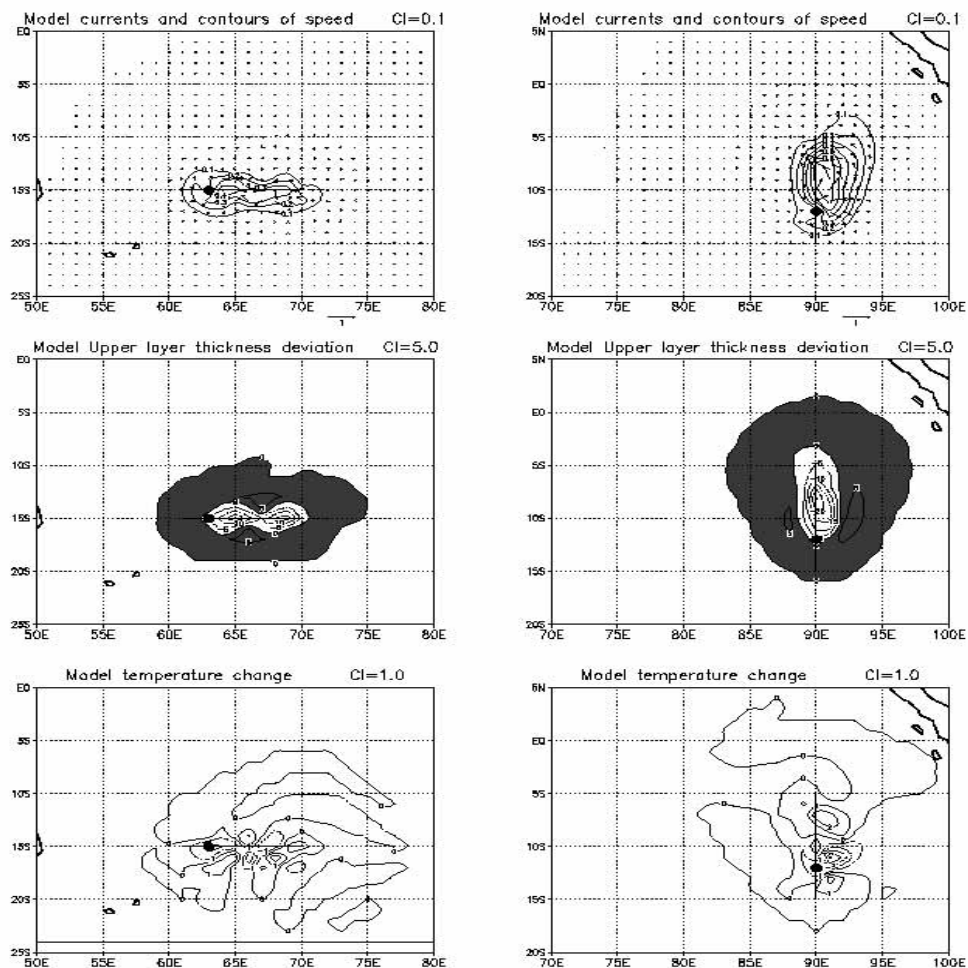


Fig.1 Model currents with contours of speed, Model upper later thickness deviation and temperature change for westward and southward track in SH for Day 4  
 ● indicates the position of the storm center on fourth day. Solid line drawn is the storm track

## The Use of Wind Gustiness and Air Density in Wave Modelling: Implementation at ECMWF

Saleh Abdalla<sup>(1)</sup> and Peter Janssen<sup>(2)</sup>

*ECMWF, Shinfield Park, Reading RG2 9AX, UK.*

<sup>(1)</sup> *e-mail: abdalla@ecmwf.int*      *Tel. +(44)(118)949 97 03*      *Fax. +(44)(118)986 94 50*  
<sup>(2)</sup> *e-mail: dax@ecmwf.int*      *Tel. +(44)(118)949 91 16*      *Fax. +(44)(118)986 94 50*

The impact and the implications of using wind gustiness and quasi-realistic air density on wave modelling have been clearly demonstrated by Abdalla and Cavaleri (2002). While air density evaluation is rather straightforward, it is not the case with the wind gustiness. There are two main approaches to include the wind speed variability in wave modelling. The first approach is the use of the Monte-Carlo simulation technique by superimposing random variability over the model (mean) wind speeds; see, *e.g.*, Abdalla and Cavaleri (2002). This approach provides instantaneous impact that may not represent the actual one. For the mean impact of gustiness, one needs to carry out several tens of realisations and average their impact. This can not be implemented in an operational set-up like the one at ECMWF. The other alternative is to replace the traditional input source term in the wave model by an enhanced form that includes the mean impact of gustiness; see, *e.g.*, Janssen (1986). Although it only provides the mean impact, this approach is more convenient for operational applications.

From the wave modelling point of view, both wind gustiness and air density affect wave generation through the wind input source term that can be written generically:

$$\frac{\partial F}{\partial t} = \gamma F \quad \text{with} \quad \gamma = \gamma \left( \frac{\rho_{air}}{\rho_{water}}, u_* \right)$$

where,  $F$  is the energy density of a wave component,  $t$  is the time,  $\rho_{air} / \rho_{water}$  is the air-water density ratio (which is usually assumed constant in wave models), and  $u_*$  is the wind friction velocity component along wave propagation direction. Usually mean wind velocity is used. This implies an ignorance of the impact of variability at scales lower than or comparable to the atmospheric model resolution. To include this impact, an enhanced input source term with the mean impact of gustiness can be estimated as:

$$\begin{aligned} \bar{\gamma}(u_*) &= \int_{u_*=-\infty}^{\infty} \frac{1}{\sigma_* \sqrt{2\pi}} \exp \left( -\frac{(u_* - \bar{u}_*)^2}{2 \sigma_*^2} \right) \gamma(u_*) du_* \\ &\cong 0.5 \left[ \gamma(\bar{u}_* - \sigma_*) + \gamma(\bar{u}_* + \sigma_*) \right] \end{aligned}$$

Here  $u_*$  represents the instantaneous unresolved friction velocity,  $\sigma_*$  is its standard deviation and the *over-bar* represents the mean value of the quantity over the whole grid-box/time-step. The second equation follows from the Gauss-Hermite quadrature. To estimate the value of  $\sigma_*$ , one can make use of the empirical expression of Panofsky *et al.* (1977) which requires the knowledge of the height of the lowest inversion and the Monin-Obukhov length. Abdalla (2001) explains this with some details.

Several experiments were carried out to test this implementation using low-resolution model (T159). The positive impact encouraged the application with the current ECMWF model resolution of T511/L60. The spatial resolution of the atmospheric model is about 40

km while that of the wave model is 55 km. The integration time step is 15 minutes. The two-way coupling between the atmospheric and the wave models is done at each time step. This set-up was run for the periods: 22 Nov.-14 Dec. 2000 and 1-27 Jun. 2001. The wave scores (anomaly correlation and standard deviation of error) of the significant wave height compared to those of the control run are shown in Fig. 1 for the 23 cases. Although the Northern Hemisphere (NH) scores are almost neutral for the first 6 days, remarkable positive impact can be seen for the Southern Hemisphere (SH). Verifying the model forecast wave heights against both the in-situ buoy and the ERS-2 radar altimeter observations further proved this impact. In general, the new implementation increases the average wave height, which is usually a positive impact to compensate for the general model tendency to have negative bias. This implementation will soon be tested in an e-suite at ECMWF.

**References:**

Abdalla, S., 2001. Impact of wind gustiness and air density on modelling of wave generation: Implementation at ECMWF, *ECMWF Workshop on Ocean Wave Forecasting*, 2-4 July 2001, ECMWF, Reading, UK.

Abdalla, S. and L. Cavaleri, 2002. Effect of wind variability and variable air density on wave modelling, *Accepted for publication in Journal of Geophysical Research*.

Janssen, P.A.E.M., 1986. On the effect of gustiness on wave growth, *KNMI Afdeling Oceanografisch Onderzoek memo 00-86-18*, 17pp., Koninklijk Nederlands Meteorologisch Instituut, De Bilt, The Netherlands.

Panofsky, H.A., H. Tennekes, D.H. Lenschow and J.C. Wyngaard, 1977. The characteristics of Turbulent velocity components in the surface layer under convective conditions, *Boundary-Layer Meteorology*, **11**, pp.355-361.

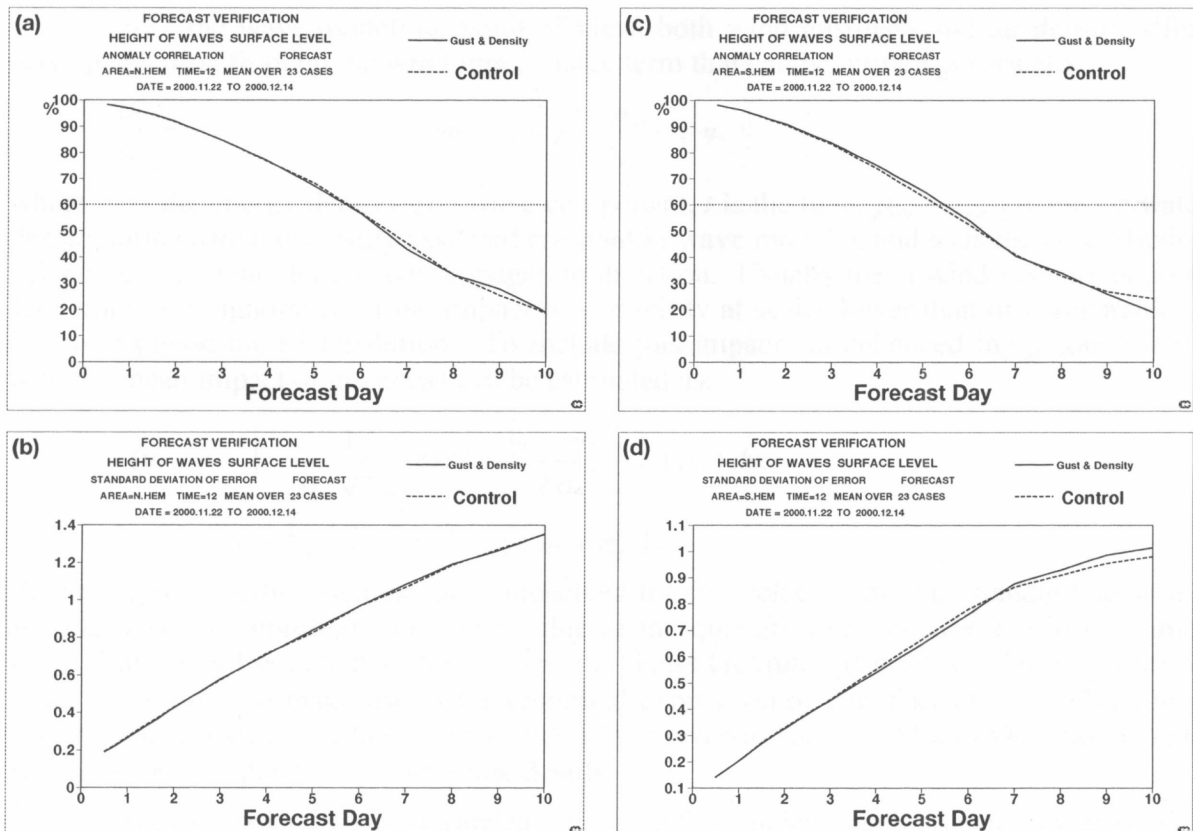


**Fig. 1:** Significant wave height scores (anomaly correlation and standard deviation of error) for 23 cases (22 Nov. - 14 Dec. 2000) for NH (panels a & b) and SH (panels c & d).

# The Use of Wind Gustiness and Air Density in Wave Modelling: Impact and Implications

Saleh Abdalla<sup>(1)</sup> and Luigi Cavaleri<sup>(2)</sup>

<sup>(1)</sup> ECMWF, Shinfield Park, Reading RG2 9AX, UK.

e-mail: [abdalla@ecmwf.int](mailto:abdalla@ecmwf.int)

Tel. +(44)(118)949 97 03

Fax. +(44)(118)986 94 50

<sup>(2)</sup> ISDGM, S.Polo 1364, 30125 Venice, Italy.

e-mail: [l.cavaleri@isdgm.ve.cnr.it](mailto:l.cavaleri@isdgm.ve.cnr.it)

Tel. +(39)(041)521 68 10

Fax. +(39)(041) 260 23 40

The impact of wind gustiness on the evolution of wave fields is analysed by superimposing to the nominal wind speed a fluctuation whose amplitude is related to the local air-sea temperature difference. The use of fluctuations represented by a Gaussian process, characterised by coherence in time, produces realistic time series whose characteristics are compatible with those obtained from previous studies and open sea measurements. To display the impact of the quasi-realistic temporal coherence, wind gustiness was represented in the wave as a Gaussian process with and without coherence in time. While a single extended simulation can provide a general idea of the impact of gustiness on the climatology, its randomness does not allow definite conclusions when one focuses on a specific location and on a given time. This effect is more pronounced in the case of coherence. An ensemble approach is used with several tens of random realisations.

The effect of a variable air density on wave generation has been explored by repeating the hindcasts using air density values estimated from the output of a meteorological model.

Table 1 summarises some of the numerical tests we carried out in the North Atlantic and the Mediterranean to display the impact of gustiness and variable air density on wave generation. Table 2 summarises the impact of gustiness without and with coherence and air density on the predicted significant wave height. Fig. 1 shows the results of the ensemble approach at buoy 64046 (located north of the UK at around 60.5°N, 5.0°W).

The introduction of gustiness leads to an evident average increase of the resulting wave heights, larger in an open ocean (the North Atlantic) than in an enclosed basin (the Mediterranean Sea). It is worthwhile mentioning that there is significant impact of gustiness during some individual storms characterised by high unstable conditions like the Mistral. This can be clearly seen in Figure 1 and inferred from the high maximum differences in Table 2. The randomness of the wind, and hence, at a more limited extent, of the wave fields implies the possible occurrence of wave heights much larger than expected in a *non-gusty* field. The impact is more pronounced in the case of gustiness with coherence in time. The quasi-realistic air density in the North Atlantic Ocean leads to an increase of the wave heights during the winter storms. This impact is much limited in the Mediterranean Sea. The details can be found in Abdalla and Cavaleri (2002).

## **Reference:**

Abdalla, S. and L. Cavaleri, 2002. Effect of wind variability and variable air density on wave modelling, *Accepted for publication in Journal of Geophysical Research.*

**Table 1:** Summary of some of the numerical tests.

Run ID	Forcing	Period	Region
AR	Reference (standard model run)	01 October 1999 - 31 March 2000	North Atlantic
AN	Gustiness without coherence		
AC	Gustiness with coherence		
AD	Variable air density		
AE	Ensemble of 50 members, gustiness with coherence	15-20 December 1999	
MR	Reference (standard model run)	01 October 1993 - 31 March 1994	Mediterranean
MN	Gustiness without coherence		
MC	Gustiness with coherence		
MD	Variable air density		
ME	Ensemble of 50 members, gustiness with coherence	21-24 October 1993 (Mistral Storm)	

**Table 2:** Gustiness and air density impact on predicted significant wave heights. The first row provides the maximum negative difference (metre), in space and time, with respect to the reference run. The second row refers to the long term average differences on the single points of the grid. The third and fourth rows provide the corresponding positive results. The columns *AR* and *MR* show the overall mean and maximum for both reference runs.

Run ID:	<i>AR</i>	<i>AN</i>	<i>AC</i>	<i>AD</i>	<i>MR</i>	<i>MN</i>	<i>MC</i>	<i>MD</i>
Max. negative diff.	----	-1.09	-2.35	-0.49	----	-0.75	-1.41	-0.37
Lowest mean	4.13	-0.00	+0.00	-0.01	1.44	-0.01	-0.00	-0.01
Highest mean		+0.07	+0.20	+0.10		+0.00	+0.03	+0.01
Max. positive diff.	14.73	+2.37	+6.59	1.09	9.57	+0.64	+2.01	+0.33

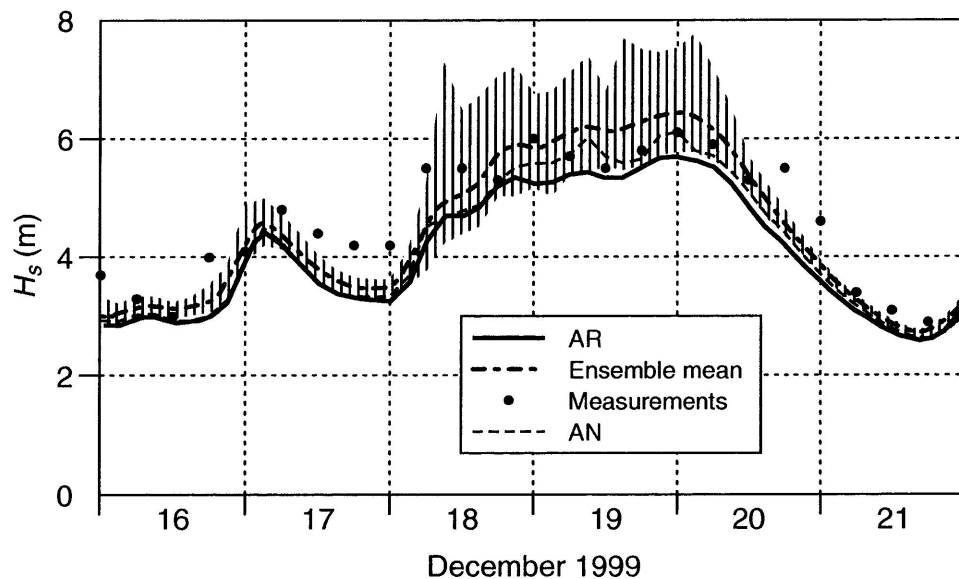


**Fig. 1:** Time history of wave height at buoy 64046 (shaded area represents envelope of AE).

# Simulation of the Red Sea Tides

A.A. Androsov, A.V. Nekracov, D.A. Romanenkov\*, N.E. Voltzinger  
*St.Petersburg Branch, Institute of Oceanology, Russian Academy of Sciences*  
*30, Pervaya Liniya, 199053 St.Petersburg, Russia*

\* Corresponding author. *E-mail addresses:* roman@gk3103.spb.edu (D.A. Romanenkov).

Modelling the tides in the Red Sea requires a satisfactory description of its complicated relief and shore line configuration (Morcos, 1970; Prat et al, 1999, 2000). Also, the local tidal characteristics may, to a considerable extent, be formed by the sharp seasonal changes of stratification with its typical structure in different parts of the Sea.

For computation of the tides in the Red Sea, a 3-D boundary-value problem for the equations of motion, continuity, temperature, salinity and characteristics of turbulence is formulated in a domain with an open boundary south of the Gulf of Aden to the northern end of the Gulf of Suez (Fig. 1).

The boundary-value problem is transformed to the boundary-fitted curvilinear coordinates. The equations in the form of contravariant fluxes are integrated by the difference method. The numerical method uses conservative schemes for the split operators, allowing one to control the scheme viscosity and the solution behavior in the locality of its sharp gradients (Androsov et al., 2002).

Below are given some results obtained in a computation of the 3-D barotropic tide for the northern part of the Red Sea and the Gulf of Suez. The boundary conditions at a cut of  $24^{\circ} N$  are found by data interpolation of the level oscillation at Stations 1 ( $35.5^{\circ} E$ ,  $23.967^{\circ} N$ ) and 13 ( $37.1^{\circ} N$ ,  $24.967^{\circ} N$ ). The horizontal curvilinear grid contains  $65 \times 69$  points for the north Red Sea and  $33 \times 129$  points for the Gulf of Suez with a step that varies from 0.4 km to 14 km. In the vertical direction, 50 horizons were used; the time step is 232.875 s. In Fig. 2, the  $M_2$ -tidal chart in the Gulf of Suez is presented. In Fig. 3, a comparison of the results with data at 11 stations for the  $M_2$ -wave computation is given. The rms error of level computation for the tidal period (12.42 h) is 1.6 cm.

**This work was supported by the Russian Foundation for Basic Research, project No. 00-05-64300.**

## *References:*

1. Morcos, S. A., 1970. Physical and chemical oceanography of the Red Sea., *Oceanogr. Mar. Biol. Ann. Rev.*, 8, 73–202.
2. L.J. Pratt, W. Johns, S.P. Murray, and K. Katsumata, 1999, Hydraulic Interpretation of Direct Velocity Measurements in the Bab al Mandab, *J.Phys.Ocean.*, **29**, 11, 2769–2784.
3. L.J.Pratt, H.E.Deese, S.P.Murray, and W.Johns, 2000, Continuous Dynamical Modes in Straits Having Arbitrary Cross Sections, with Applications to the Bab al Mandab, *J.Phys.Ocean.*, **30**, 10, 2515–2534.
4. A. A. Androsov, N. E. Voltzinger, and D. A. Romanenkov, 2002, Simulation of Three-Dimensional Baroclinic Tidal Dynamics in the Strait of Messina, *Izvestiya RAN, Atmospheric and Oceanic Physics*, **38**, 1.

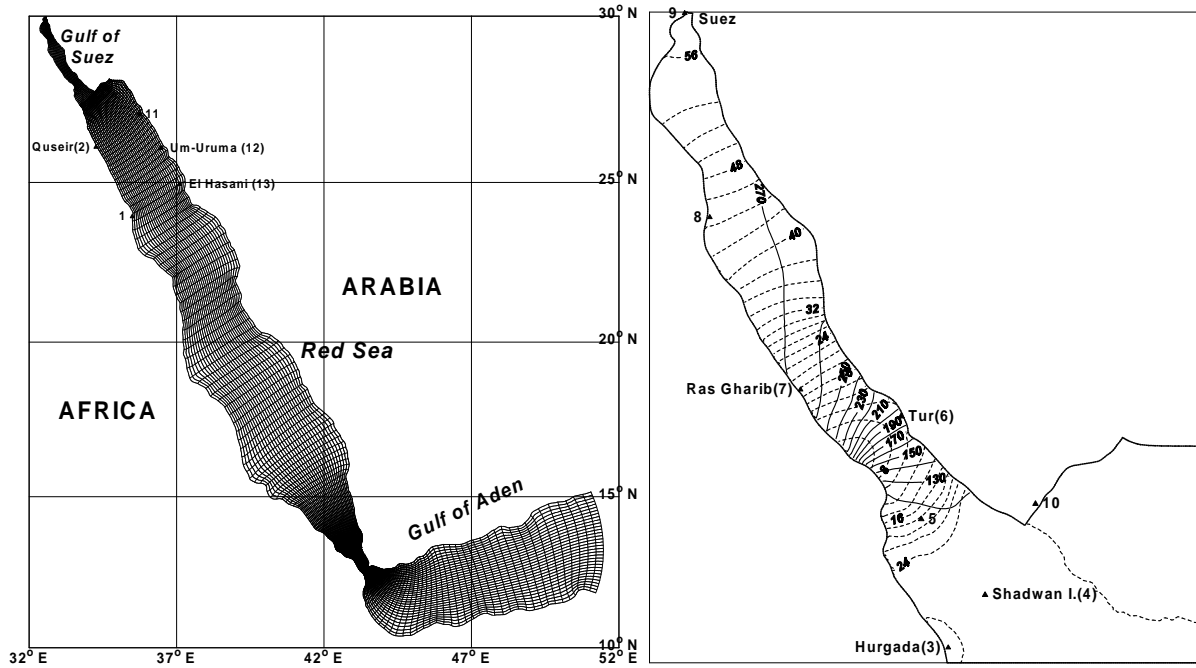


Figure 1: Curvilinear grid of the Red Sea and the Gulf of Aden. The grid is coarsened for illustration.

Figure 2:  $M_2$ -tidal map of the Gulf of Suez. Isophases (in deg.) — ; isoamplitudes (in cm) - - -.

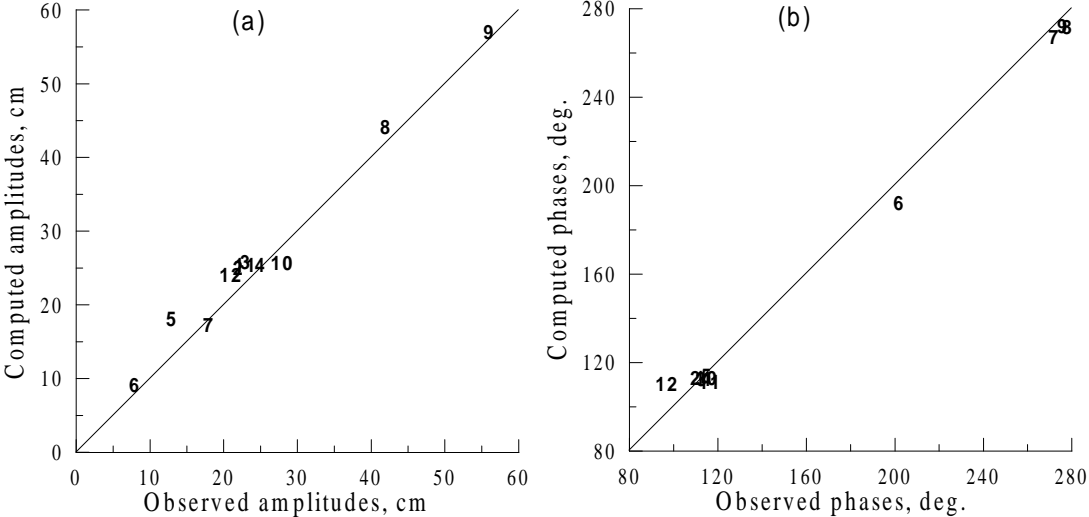


Figure 3: Correlation between the data and computed values of amplitudes and phases of the sea-level oscillations for the  $M_2$ -constituent; (a) – amplitudes, (b) – phases. Stations location see in Fig. 1 and Fig. 2.

## **The Forecasting Ocean Assimilation Model (FOAM) System**

M. J. Bell, A. Hines, P. Holland,  
M. J. Martin, M. E. McCulloch and D.  
Storkey

Met Office, London Rd, Bracknell,  
Berks, RG12 2SZ, U K.

Email: mike.bell@metoffice.com

### **Introduction**

The aim of the FOAM system is to provide real-time, operational, analyses and forecasts of the three-dimensional structure of the deep ocean and of sea-ice. The ocean fields that are forecast are the temperature, salinity, currents and mixed layer depth. The concentration and depth of sea-ice are also forecast. The primary objectives are to forecast the surface mixed layer to 3-5 days ahead and the mesoscale structure (perhaps up to 10-20 days ahead).

A global version of the FOAM system has run each day in the Met Office's operational suite since it was introduced in 1997. The system is described in detail in Bell et al. (2000). It is based around a z co-ordinate, primitive equation ocean model on a grid with 1° spacing in the horizontal and 20 levels in the vertical. The model is forced by 6-hourly surface fluxes from the Met Office's numerical weather prediction (NWP) system and assimilates thermal profile and surface temperature data. This report outlines the main developments made to the system since 1997.

### **Development of Hindcast and Rapid Response Nested Model Capabilities**

An accessible archive of 6-hourly surface fluxes from the Met Office's NWP system has been established back to May 1996. The suite control system (SCS) used for operational NWP is used for the FOAM operational forecasts and for long period (e.g. 3 year) hindcasts, using the 6-hourly fluxes, to test new versions of the FOAM system.

The facility to nest higher resolution, limited area models inside lower resolution larger area models has been developed. The nesting is one-way and uses the flow relaxation scheme (Davies 1983). A model covering the Atlantic and Arctic oceans with a 35-km grid was added to the operational suite in January 2001.

A system to set up new model configurations, to spin them up to real-time, and to produce daily pre-operational forecasts has been developed and used to support the Royal Navy's Saif Sareea exercise in the Arabian Sea using models covering the Arabian Sea with a 13 km grid and the Indian Ocean with a 35 km grid nested inside a 1° global model.

The dependence of the model integrations on the choice of harmonic and biharmonic viscosities, thermal diffusivities and upwind advection schemes has been explored in models of widely varying horizontal resolutions.

A model covering the North Atlantic with a 13-km grid has been established. After 1 year of integration the separation of the flow at Cape Hatteras is good given the resolution (see figure), though the separated path appears to be too variable.

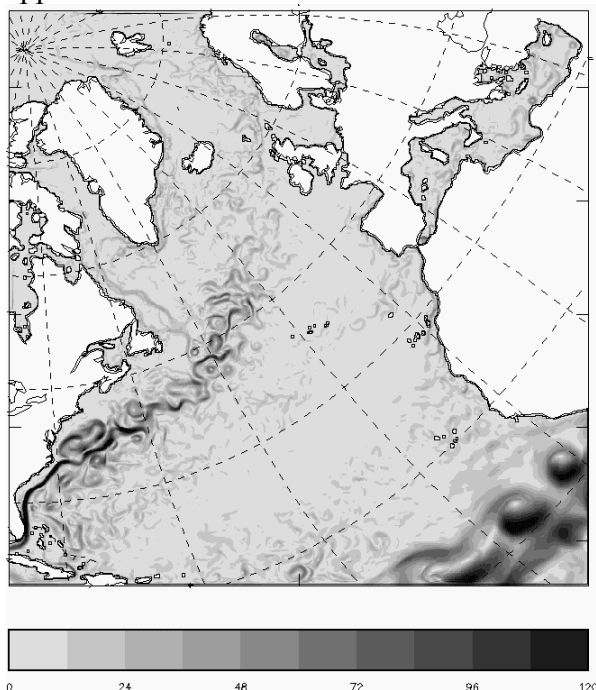


**Figure:** Five-day mean surface current speeds (cm/s) in North Atlantic FOAM model after 15 months of spin up using monthly mean fluxes and no data assimilation

### Developments to observations assimilated

Fields of sea-ice concentration received from the Canadian Meteorological Center have been assimilated into the FOAM operational model since 6 July 1999.

The FOAM group has experimented with the assimilation of altimeter data for many years. Routine (weekly) delivery of altimeter data from CLS (Centre Localisation Spatiale) in Toulouse however was only

established in August 2001. These data have been assimilated in the operational Atlantic model since 25<sup>th</sup> Sept. 2001.

Developments to the techniques used for data assimilation are described in a separate contribution.

### Distribution of products and GODAE

Gridpoint data from the operational FOAM system are available through the Met Office's Data Products Distribution Server (DPDS). During the main phases of the Global Ocean Data Assimilation Experiment, gridpoint data from high resolution FOAM systems run on a daily pre-operational basis will be available through the Live Access Server at <http://www.nerc-essc.ac.uk/las>

### References

- Bell, M. J., R. M. Forbes, A. Hines 2000 Assessment of the FOAM global data assimilation system for real-time operational ocean forecasting. *J. Mar. Sys.*, 25, 1-22.
- Davies, H. C. 1983 Limitations of some common lateral boundary schemes used in regional NWP models. *Mon. Weather Rev.*, 111, 1002-1012.

## **Developments to the Data Assimilation Methods used by the Forecasting Ocean Assimilation Model (FOAM) System**

M. J. Bell, A. Hines and M. J. Martin

Met Office, London Rd, Bracknell,  
Berks, RG12 2SZ, U K.

Email: mike.bell@metoffice.com

### **Introduction**

The aim of the FOAM system is to provide real-time, operational, analyses and forecasts of the three-dimensional structure of the deep ocean and of sea-ice. A global version of the FOAM system has run each day in the Met Office's operational suite since it was introduced in 1997. The data assimilation scheme originally employed is described in detail in Bell et al. (2000). It assimilated thermal profile and surface temperature data using the analysis correction scheme devised by Lorenc et al. (1991). The accompanying report describes the development of high-resolution nested FOAM models and new data sources.

### **Tuning of Assimilation of Surface Data**

The dependence of the assimilation of altimeter data based on the Cooper & Haines (1996) scheme in models with grid spacing between 100 km and 13 km on several factors has been investigated (Hines 2001). The correlation scales, time-mean surface height and quality control measures used all had significant impact on the results. Subsequent work has shown the lifting and lowering of model profiles to be detrimental in the mixed layer

Similar investigations of the assimilation of surface temperature data have been made. Best results were obtained using forecast error covariances containing a broad range of spatial scales and making bias corrections to the satellite data using the in situ observations.

### **More timely assimilation of data**

Observations retain their relevance to ocean analyses for many days. A method has been devised for making increments to the model fields close to the time of validity of each observation and thereafter giving additional weight to the model field according to the estimated retention of information from the observation. This method enables observations to be fully assimilated on the day that they arrive and does not require assimilation cycles to be repeated. The derivation of the method is described in detail in Bell et al. (2002).

### **Improved estimates of the forecast error covariance**

We suspect that there are two main sources of errors in our ocean models and that they have distinctly different scales and characteristics: errors in the surface forcing with atmospheric "synoptic" scales; and errors resulting from mislocation of internal ocean "mesoscale" instabilities. Using data from a 3 year hindcast of our Atlantic model (35 km grid spacing) we have estimated the model error covariances as functions of the separation distance using pairs of observation minus forecast values and represented them as the sum of two second order auto-

regressive (SOAR) functions. For surface height and temperature data the variances and correlation scales can be estimated for  $10^{\circ}$  grid boxes. The two correlation scales derived are clearly separated and vary quite smoothly with location. The synoptic scale variances depend little on geographical location but the mesoscale variances vary by orders of magnitude, being largest in the western boundary current regions. Information on the vertical dependence of temperature variances and the horizontal and vertical correlation scales have been estimated from profile observations for each component but as yet only as basin averages. The dependence on depth of the variance of vertical isopycnal displacements has also been calculated (as basin averages) from the thermal profile data.

### **A Bias Correction Scheme**

Assimilation of thermal data near the equator was found to generate spurious vertical motions. A method for producing more balanced analyses is suggested in Bell et al. (2001).

### **References**

- Bell, M. J., R. M. Forbes, A. Hines 2000 Assessment of the FOAM global data assimilation system for real-time operational ocean forecasting. *J. Mar. Sys.*, 25, 1-22.
- Bell, M. J., M. J. Martin, and N. K. Nichols 2001 Assimilation of data into an ocean model with systematic errors near the equator. *Ocean Applications Tech. Note No. 27*. Available from Met Office, Bracknell, UK.
- Bell, M. J., M. J. Martin, and A. Hines 2002 Variational assimilation evolving individual observations and their error estimates. To be submitted.
- Cooper M., and K. Haines 1996 Data assimilation with water property conservation. *J. Phys. Oceanogr.*, 101, 1059-1077.
- Hines, A. 2001 Implementation and tuning of altimeter data assimilation scheme for high-resolution FOAM models. *Ocean Applications Technical Note No. 26*. Available from Met Office, Bracknell, UK.
- Lorenc, A. C., R. S. Bell, B. Macpherson 1991 The Meteorological Office analysis correction data assimilation scheme. *Quart. J. Roy. Meteor. Soc.*, 117, 59-89.

# Impact of Different surface winds on SST in the north Indian Ocean

D. W. Ganer, A. A. Deo, P. S. Salvekar and K. Annapurnaiah  
Indian Institute of Tropical Meteorology, Pune-411008, India.  
E-mail : tsd@tropmet.ernet.in

## Introduction

The annual reversal of the monsoon wind changes the behaviour of the upper north Indian ocean. The strong southwesterly winds during the monsoon season plays an important role in cooling the sea surface. The small change in SST may cause large-scale ocean-atmosphere phenomena similar to that in the tropical Pacific. The different surface forcings also produce some changes in the simulation of the SST. Therefore an attempt is made in this study to simulate SST using thermodynamic ocean model with two different wind stresses.

## The Model and input

In the present work 2½ layer thermodynamic ocean model over the region 35 °E-115 °E, 30 °S - 25 °N is used which is fully described in McCreary et al.(1993, MKM) and Behera et al.(1998). The model has two active layers overlying a deep motionless layer of infinite depth. The surface layer separates into two sub-layers i.e. a well mixed upper turbulent layer and a non-turbulent fossil layer through entrainment and detrainment. The uppermost sub-layer is considered as model mixed layer and its temperature is considered as the representative of model SST. For details of the model readers may refer to MKM. The model is spun up for ten years to reach steady state using ten years monthly mean climatology (1983-1992) of NCEP and COLA T30 L18 AGCM winds(Center for Ocean-Land-Atmosphere). The model integration is further carried out with inter-annually varying monthly winds of NCEP and COLA . In both cases the NCEP heat flux is used as a thermal forcing.

## Results and discussion

The simulated SSTs in both the wind cases are in the range of 21°C to 30°C. The difference between the Reynolds SST and the model SST in NCEP case is 0.5°C in all the months and are in agreement with Behera et al, 2000. The simulated SSTs for the year 1985 (Fig. not shown) which is a bad monsoon year in both the cases differ less as to that of year 1986 . Figure 1 shows the difference between the SSTs simulated in both the cases for the year 1986 at bimonthly interval. The comparison of model SST from COLA wind and that of NCEP wind shows difference of about 1°C to 2°C during May to August north of 10S. This suggests that the heat fluxes are more dominant in simulating the SST south of 10S. The cooling of about 1-2°C is found in western equatorial Arabian Sea and western Bay of Bengal in COLA wind case suggest strong wind stress during May to August.

## References

- Behera S K, Salvekar P S, Ganer D W, 1999: Numerical investigation on wind induced interannual variability of north Indian Ocean SST, *IITM Research Report* No. RR-085.
- McCreary J P, Kundu P K and Molinary R L, 1993: A numerical investigation of dynamics, thermodynamics and mixed layer processes in the Indian Ocean; *Prog. Oceanogr.*, **31**, 181-244.
- Behera S K, Salvekar P S and Yamagata T, 2000: Simulation of Interannual SST variability in the tropical Indian Ocean; *Journal of Climate*, 3487-3499.

## Acknowledgement

Authors are thankful to CGMD members of IITM to provide COLA winds used in this work. This work is carried out on SUN Ultra 60 workstation, which is acquired under DOD project.

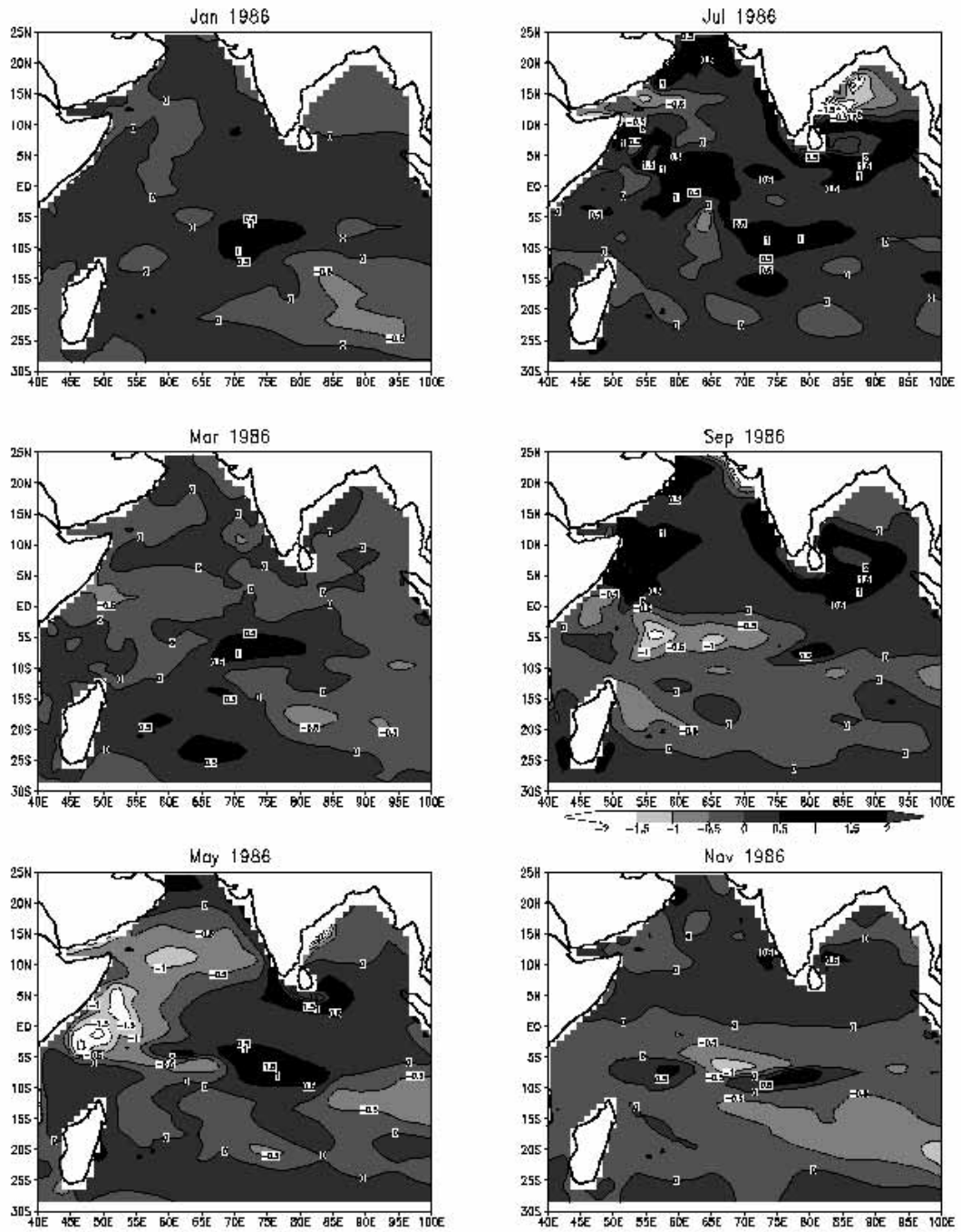


Fig.1 Difference between model SSTs using COLA & NCEP winds

# Development of a High Resolution Ocean Model for ENSO Forecasting

Naoyuki Hasegawa

n-hasegawa@met.kishou.go.jp

Japan Meteorological Agency

1-3-4, Otemachi, Chiyodaku, 100, Tokyo Japan

## 1. Introduction

The Japan Meteorological Agency (JMA) operates a coupled ocean and atmosphere model for the ENSO prediction. The oceanic part of this model is identical to that used in the Ocean Data Assimilation System (Kimoto et al., 1997), which provides the oceanic initial conditions for the coupled model. A high resolution version of this ocean model was developed to assess the impact of the resolution on the model performance.

## 2. Model

The horizontal resolution was enhanced from 2.0° latitude (0.5° between 10°S and 10°N) by 2.5° longitude to 1.25° latitude (0.25° for 10°S -10°N) by 1.25° longitude. The model was modified from a rigid lid model which follows Bryan (1969) to a free surface model based on Killworth et al. (1991) to avoid the solution of a Poisson-type equation. The vertical resolution was also improved from 20 levels to 30 levels and the layer spacing around the equatorial thermocline was reduced from 30m to 15m. The models have realistic bottom topography, but the maximum depth of the bottom is set to 4000 meters. The computational domain is global, excluding the Arctic Ocean.

In a  $z$ -coordinate free surface model, when the thickness of the top layer is less than the range of the sea surface displacement (2 to 3 m), the sea surface may be moved beyond the bottom of the top layer, and this would cause the complication in the algorithm. Therefore, a new vertical coordinate was introduced in the high resolution model. The vertical coordinate  $\zeta$  is defined as;

$$z = z_0 \left( \frac{z + dh}{z_0 + dh} \right), \text{ where } \begin{cases} d = 1 & (z < z_0) \\ d = 0 & (z \geq z_0) \end{cases} \text{ (see Fig. 1)}$$

Note that  $z$  and  $\zeta$  are in the downward direction and  $\eta$  (sea surface displacement) is in the upward.  $z_0$  is set to be a depth above which no bottom topography is present (e.g. 50m). This coordinate allows the top layer to be very thin (1.6m in the high resolution model), while keeping the virtue of the  $z$ -coordinate in the pressure gradient calculation. This modification of the dynamical frame was found not to give significant difference in the performance when run at the same resolution as the present model.

The both models employ the vertical mixing of Pacanowski and Philander (1981). A Smagorinski-type second order horizontal diffusion is used in the present model and the high resolution model has the forth order horizontal diffusion with a constant diffusion coefficient.

## 3. Experiment

The impact of the resolution was assessed by integrating the present and the high resolution models with fluxes based on observation from 1980 to 1996. After 15 year spinup runs with climatological wind stress and restoring force to the climatological SST, the models were given the fluxes calculated from the atmospheric fields of the European Centre for Medium-Range Weather Forecasts (ECMWF) reanalysis (provided to JMA by courtesy of ECMWF) and JMA operational atmospheric analysis (1994-1996). The short and long wave radiation fluxes were based on Reed (1977) and Budyko (1974), respectively. The momentum, latent heat and sensible heat fluxes were calculated with the formulae given by Bunker (1976). The cloudiness in the calculation was estimated from the relative humidity with a statistical relation by

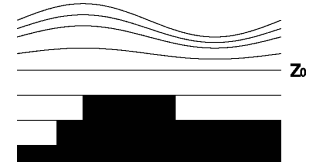


**Fig.1** Vertical coordinate used in the high resolution model.

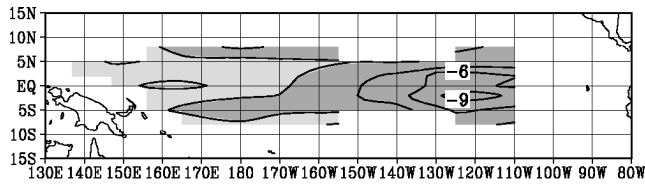


**Fig.2** Difference of RMSEs of 5 day mean 20°C depth for 1984-1996 (m). Dark shade indicates the negative difference (high resolution is better) and light shade indicates the positive difference. The contour interval is 3m.

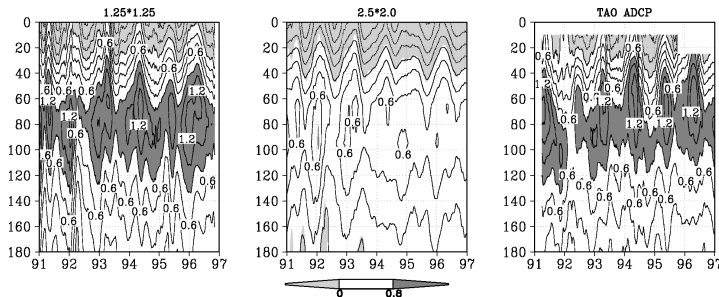


**Fig.3** Time- depth diagram of the eastward currents at 0°N, 110°W (m/s) from January 1990 to December 1996 for the high resolution model (left), the present model (center) and TAO ADCP (right).

#### 4. Results

When compared with the TAO data, the models showed warm SST bias (around 1°C) in the equatorial Pacific, and its magnitude was not reduced by the high resolution model (figures not shown). However, some improvements were seen in the subsurface structure, which is important for ENSO prediction. The high resolution model gave better thermocline depth (20°C depth) in the eastern equatorial Pacific (Fig. 2). This was mostly brought about by the reduction of the deepening bias of the 20°C depth in the low resolution model. The high resolution model also gave better (sharper) vertical temperature gradient within the thermocline (figures not shown). The present model gave substantially weaker Equatorial Undercurrent, but this was remedied by the high resolution model (Fig. 3). The high resolution model reproduced the tropical instability waves (Legeckis, 1977, etc.) which was absent in the present model (Fig. 4), though the effect of this wave on ENSO is yet to be studied.

#### REFERENCE

- Bryan, K., 1969: A numerical method for the study of the circulation of the world ocean. *J. Comput. Phys.*, **4**, 347-376.
- Budyko, M. I., 1974: *Climate and Life*. Academic Press, 508pp.
- Bunker, A. F., 1976: Computations of surface energy flux and annual air-sea interaction cycles of North Atlantic Ocean. *Mon. Wea. Rev.*, **104**, 1122-1140.
- Killworth, P. D., D. Stainforth, D. J. Webb and S. M. Paterson, 1991: The development of a free-surface Bryan-Cox-Semtner ocean model. *J. Phys. Oceanogr.*, **21**, 1333-1348.
- Kimoto, M., I. Yoshikawa, and M. Ishii, 1997: An ocean data assimilation system for climate monitoring. *J. Meteor. Soc. Japan*, **75**, 471-487.
- Legeckis, R., 1977: Long waves in the eastern equatorial Pacific Ocean. *Science*, **197**, 1179-1181.
- Pacanowski, R. and S. G. H. Philander, 1981: Parameterization of vertical mixing in numerical models of tropical oceans. *J. Phys. Oceanogr.*, **11**, 1443-1451.
- Reed, R. K., 1977: On estimating insolation over the ocean., *J. Phys. Oceanogr.* **7**, 854-871.
- Saito, K. and A. Baba, 1988: A statistical relation between relative humidity and the GMS observed cloud amount. *J. Meteor. Soc. Japan*. **66**, 187-192.

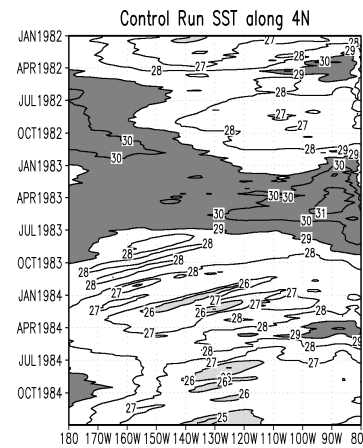


**Fig.4** Time-longitude diagram of the SST (°C) along 4°N by the high resolution model from Jan. 1982 to Dec. 1984.

Saito and Baba (1988). The model SST was used in the flux calculation. Salinity was restored to the climatology for all the model runs. The temperatures were restored to the climatology in the entire region for the first 10 years of the spinup and below 1500m and poleward of 50° for the rest of the experiment.

The relationship between monthly mean SLP and mean wave height is obtained from the CCA shows Fig. 2. Reduced pressures over the North Atlantic and Northern Europe indicate more low pressure systems in this region and this indicates increased mean wave heights. The simulated results and the observed time series are shown in figure 3.

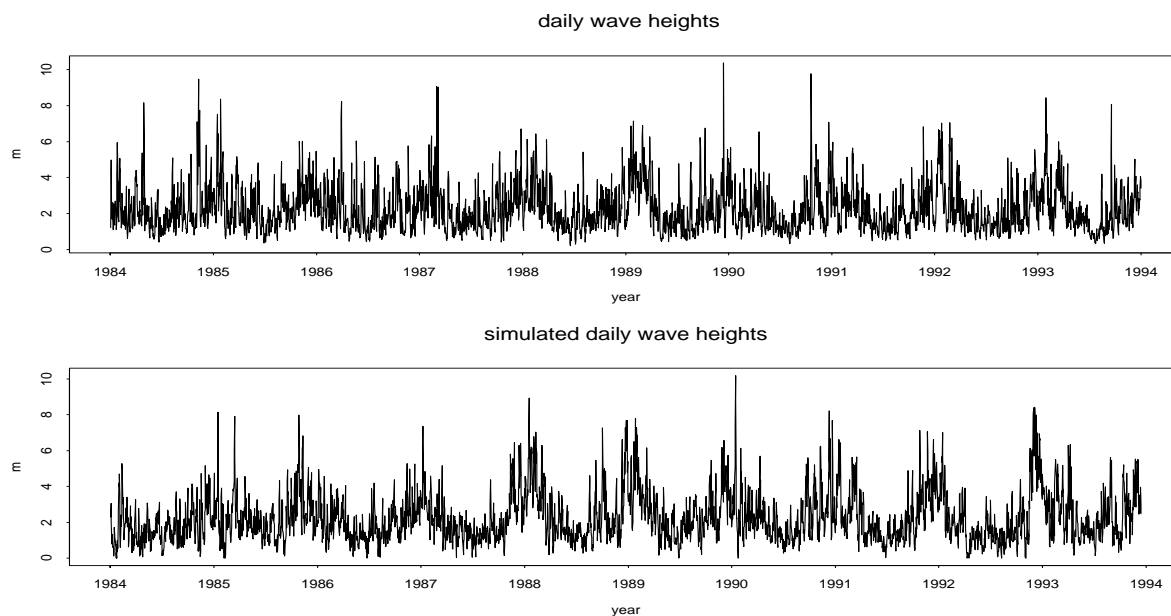


Fig.3: Observed and simulated daily wave heights (1.1.1984 - 13.12.1993)

Using diagnostics such as autocorrelation functions, quantiles, spectrum and distribution functions the wave generator was quite successfully validated against the observed wave statistics in the independent period. Figure 4 shows a quantiles - quantiles plot, Fig. 5, the comparison for the spectrum resolving periods up to 400 daysa quantiles - quantiles plot.

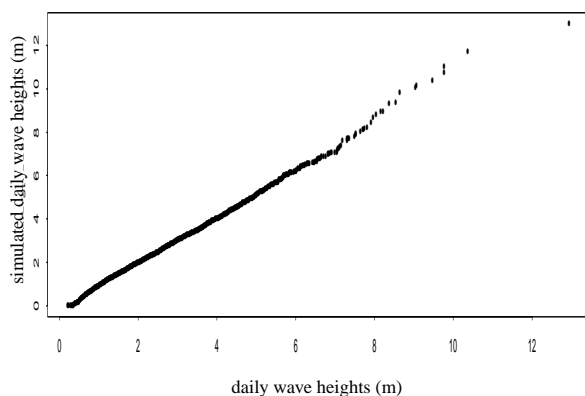


Fig. 4: Quantiles - Quantiles Plot of observed and simulated daily wave heights (1.1.1974 - 31.12.1994)

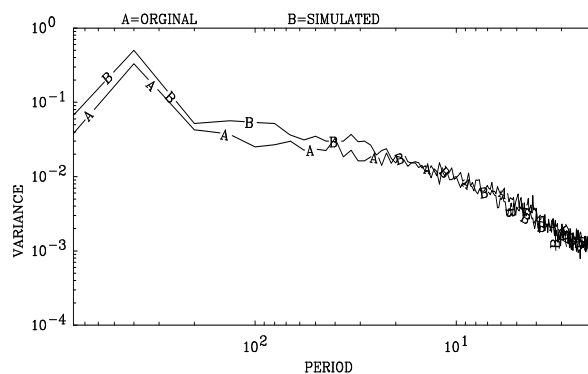


Fig. 5: Comparison of original and simulated spectrums. Periods up to 400 days.

## Reference

- Bürger, G.**, 1996: Expanded downscaling for generating local weather scenarios.in: Climate Resarch, Vol.7, 111-128.
- von Storch, and F.W.Zwiers**, 1998: Statistical Analysis in Climate Research. Cambridge University Press, in press.
- The WASA Group**, 1998: Changing Waves and Storms in the North Atlantic? in: Bulletin of the American Meteorological Society, 79, No.5, 741-760.

# Impacts of Satellite Scatterometer – Derived Wind Forcing on the West Florida Shelf Ocean Circulation

Steven L. Morey<sup>1</sup>, Mark A. Bourassa, Xujing Jia, James J. O'Brien, and Jorge Zavala-Hidalgo  
The Center for Ocean - Atmospheric Prediction Studies, FSU

A deficiency in regional to coastal scale ocean modeling is the availability of wind forcing products that accurately represent energetic weather systems. These tropical and extratropical storms have a profound impact on the upper ocean circulation, particularly in shallow regions. This research explores methods of using data from the Seawinds scatterometer aboard the QuikSCAT satellite to force a regional ocean model. A numerical simulation of the Gulf of Mexico using the Navy Coastal Ocean Model (NCOM) [Martin, 2000] is forced with three different wind data sets, the Eta-29 numerical weather prediction model, an objectively gridded scatterometer data set, and a hybrid of the two products. The ocean model solution over the West Florida Shelf (WFS) is compared to observations for the time period of August - September, 1999, which includes the passage of Tropical Storm Harvey. The WFS is chosen as a testbed for the study of the impacts of these wind products because it has been shown that the circulation in this region is dominantly controlled by the local wind stress [Weisberg, et al., 2001]. The model to data comparisons yield information about how the modeled ocean responds to the wind forcing. The results are used to evaluate a new approach to using winds measured from a polar orbiting satellite scatterometer to force regional or coastal ocean models.

The NCOM is a three-dimensional primitive equation hydrostatic ocean model developed at the Navy Research Laboratory. The model's hybrid sigma (terrain following) and z (geopotential) level vertical coordinate is useful for simulating upper ocean processes in domains encompassing both deep ocean basins and very shallow shelves. The Gulf of Mexico simulation domain encompasses entire Gulf of Mexico and Caribbean north of Honduras (15° 30' N) to 80° 36' W with 1/20° between like variables on the C-grid, 20 sigma levels above 100 m and 20 z-levels below 100 m to a maximum depth of 4000 m. The model is forced by 30 rivers discharging freshwater with monthly climatology flow rates, transport through the open boundary (with monthly climatology temperature and salinity) yielding a mean transport through the Yucatan Strait of approximately 30 Sv, monthly climatological heat flux and 12-hourly winds.

Three gridded wind products are used to force the ocean model: the 29 km Eta model 10 m winds, QuikSCAT winds objectively mapped to a 1/2° grid using winds from the same scatterometer data to create a background field, and another mapping of the QuikSCAT winds using the Eta winds as the background field. The scatterometer winds are objectively gridded using the variational method described by Pegen *et al.* [2000] (Figure 1).

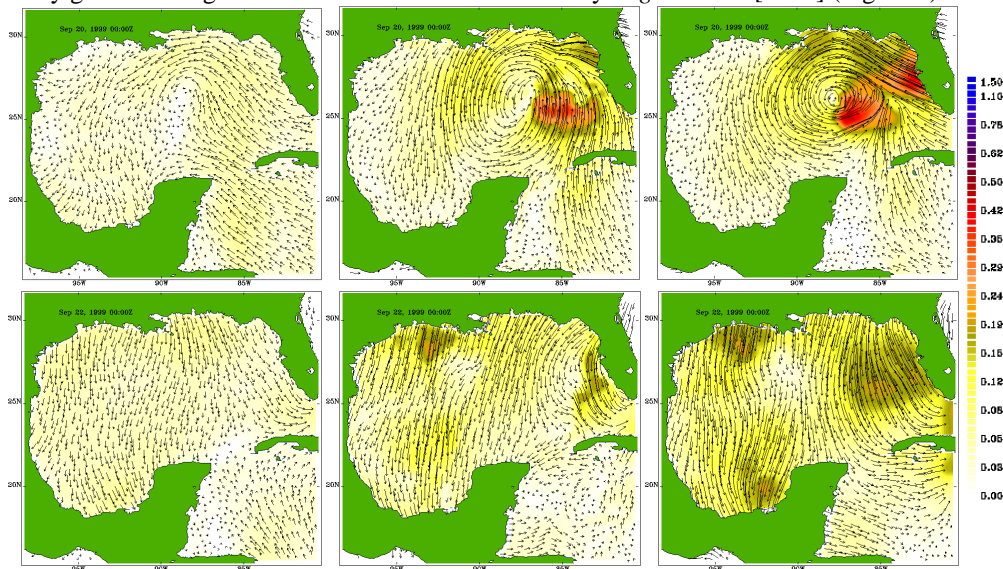


**Figure 1.** Wind stress (Pa) fields from the Eta model (left), gridded QuikSCAT winds (middle) and gridded QuikSCAT winds with the Eta background field (right) before (top) and after (bottom) T.S. Harvey passed eastward over the WFS.

<sup>1</sup> morey@coaps.fsu.edu

The hybrid QuikSCAT/Eta winds have a complex correlation magnitude of  $r=0.92$  with winds from the National Data Buoy Center buoy 42036 situated west of Tampa, FL. The Eta and QuikSCAT fields have  $r=0.85$  and  $r=0.84$ , respectively. The phase angles of the complex correlations of each wind product with the buoy are less than  $8^\circ$ . The hybrid winds have a mean wind speed 10% greater than the height adjusted buoy wind speed, and the Eta and QuikSCAT mean wind speeds are 2% greater and 26% less, respectively, than the buoy measured winds.

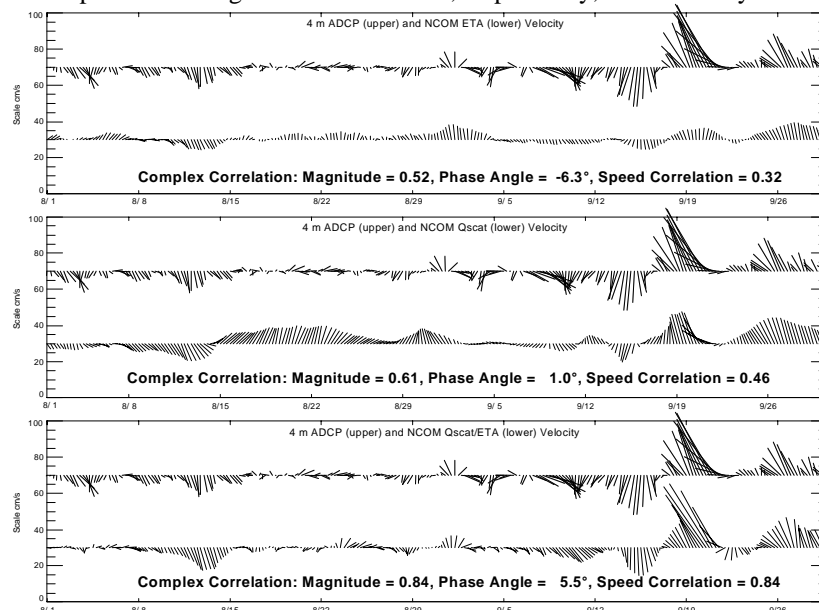


**Figure 2.** Vector velocity at 4 m depth from the COMPS CM23 ADCP (upper vectors) and NCOM (lower vectors) forced by the Eta (top), QuikSCAT (middle) and Hybrid Eta/QuikSCAT (bottom) winds.

The NCOM is validated against ADCP data from the University of South Florida Coastal Ocean Monitoring and Prediction System (COMPS) mooring CM23 located at the 50 m isobath west of Tampa (Figure 2). Results show that the NCOM velocities from the simulation forced by Eta winds do not compare well with the measured velocities. The simulation forced by the QuikSCAT winds has more reasonable velocity magnitudes, but shows an extended period of anomalously northward velocity during the second half of August. The simulation forced by the hybrid QuikSCAT/Eta winds performs best with both vector velocity and linear speed correlation coefficients of 0.84 compared to the ADCP data.

The use of the satellite scatterometer data can improve the accuracy of the winds used to force a regional scale ocean model by capturing well the spatial structure of the wind field. The frequency of the band-like sampling is, however, low (12 to 24 hours) compared to the output from the numerical weather prediction models (3 hours) so that problems may occur sampling rapidly moving storms. Using the atmospheric model data as a background field reduces the impact of spurious features that may occur when using the smoothed scatterometer data as the background field in the gridding process.

## References

- Weisberg, R.H., Z.J. Li, and F. Muller-Karger, West Florida Shelf response to local wind forcing: April 1998, *J. Geophys. Res.*, 106, 13239-262, 2001.
- Martin, P.J., "A description of the Navy Coastal Ocean Model Version 1.0". NRL Report: NRL/FR/7322-009962, Naval Research Laboratory, Stennis Space Center, MS, 39 pp., 2000.
- Pegion, P.J., M.A. Bourassa, D.M. Legler, and J.J. O'Brien, Objectively derived daily "winds" from satellite scatterometer data. *Mon. Wea. Rev.*, 128, 3150-3168, 2000.

## Acknowledgements

We thank Drs. Paul Martin, Alan Wallcraft, and others at the Navy Research Laboratory for their development of and assistance with the Navy Coastal Ocean Model. Drs. Robert Weisberg and Mark Luther at the University of South Florida graciously provided the COMPS ADCP data. Simulations were performed on the IBM SPs at Florida State University and the Naval Oceanographic Office. Computer time was provided by the DoD High Performance Computing Modernization Office. This project was sponsored by funding provided by the DoD Distributed Marine Environment Forecast System and by the Office of Naval Research Secretary of the Navy grant awarded to Dr. James J. O'Brien. NASA support came through funding for the Ocean Vector wind Science Team. Frank Wentz at Remote Sensing Systems produced the scatterometer data.

# A conditional first-order autoregressive wave-generator

Arnt Pfizenmayer and Reiner Schnur

Institute of Hydrophysics, GKSS Research Centre, Germany, email: pfiz@gkss.de

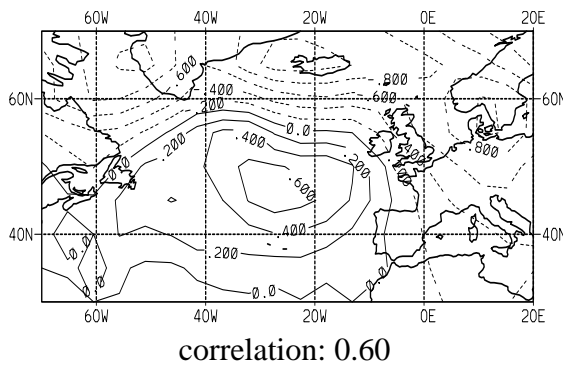
A statistical model was developed, that describes the daily wave statistics at one selected location in the North Sea was developed. With its help we can produce synthetic time series for Climate Impact studies.

As input data we used observed daily sea level pressure (SLP) over the North Atlantic and Europe and daily wave heights (1954-1994) at one selected grid point in the North Sea from a 40-year hindcast performed in the WASA project (WASA group, 1998).

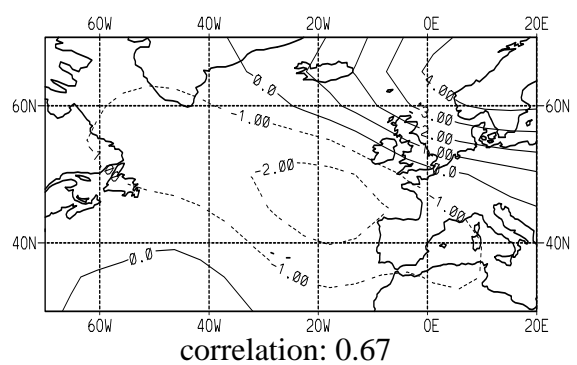
To produce time series of wave heights we used an autoregressive first-order model

$$W(t) = aW(t-1) + b(t')e(t) \quad (1)$$

(ar[1]model) (1). Where  $W$  is the wave height,  $a$  is the autocorrelation,  $b$  the estimated variance,  $e$  a random time series with normal distribution  $N(1,0)$ ,  $t$  daily time steps and  $t'$  the seasonal cycle. To fit the model we need to transform our observed data to a normal distribution. After subtracting the seasonal cycle of the data we transformed them to a normal distribution via Probability Integral Transformation (Bürger, 1996). In the fitting period (1955-74) we found a constant autocorrelation parameter (0.61), a seasonal cycle for the estimated variance and also monthly anomalies of the estimated variance. With statistical downscaling technique (CCA, v. Storch, 1998) we found a relationship between the monthly standard deviation of the highpass filtered (5 days) daily SLP and the monthly anomalies of the variance for daily wave heights. (Fig. 1) for winter (DJF). The SLP-pattern shows less variability over the North Sea and a contemporaneous decrease of the wave variance. The resulting improvement is marginal, so



-0.44



0.47

Fig.1: CCA-pattern for the monthly stdv of high pass filtered daily SLP and the estimated monthly variance of an ar[1] model for daily wave heights.

Fig.2: CCA-pattern for monthly mean SLP and the monthly mean wave height

was not integrate into the results showing here.

After retransforming our time series from normal distribution to the original distribution we add the seasonal cycle and the intra-monthly anomalies of mean wave height (2). There  $W$  is the

$$W = [W_s + W_{s'}] + W(t) \quad (2)$$

resulting wave height,  $W(t)$  the retransformed wave height from the ar[1] model,  $W_s$  the seasonal cycle and  $W_{s'}$  the monthly anomalies of wave height.

NUMERICAL INVESTIGATION OF THE INTERNAL-WAVE TRANSFORMATION  
DURING EXPANSION OF THE DEEP WATER FROM THE OPEN SEA  
TO THE SHELF BY M2 TIDAL FORCING

**Arkadiy S. Safray and Igor V. Tkatchenko\***

P.P.Shirshov Institute of Oceanology, Russian Academy of Sciences,  
St. Petersburg Branch, 30, 1-st Linia V.O., 199053, St. Petersburg,  
RUSSIA

\*Corresponding author. E-mail: [tkat@gk3103.spb.edu](mailto:tkat@gk3103.spb.edu)

To investigate the internal wave transformation during expansion of the deep water from the open sea to the shelf by M2 tidal forcing the 3-D model of marginal sea have been used. The model includes non-hydrostatic system of primitive equations of motion, equations of continuity, temperature, salinity, and constructed from them equation for pressure with co-called “artificial compressibility” and is completed with equation of state and  $k-\epsilon$  closure. The last one is a modification of Mellor' turbulent model with equation for fluctuations of temperature. Numerical approximation of the equations of the model is based on tetrahedron finite element mesh and has the 2-nd order of accuracy in time and space both. Near the shelf zone the nest grid was thickened up to 4 m in the horizontal and 1 m in the vertical direction.

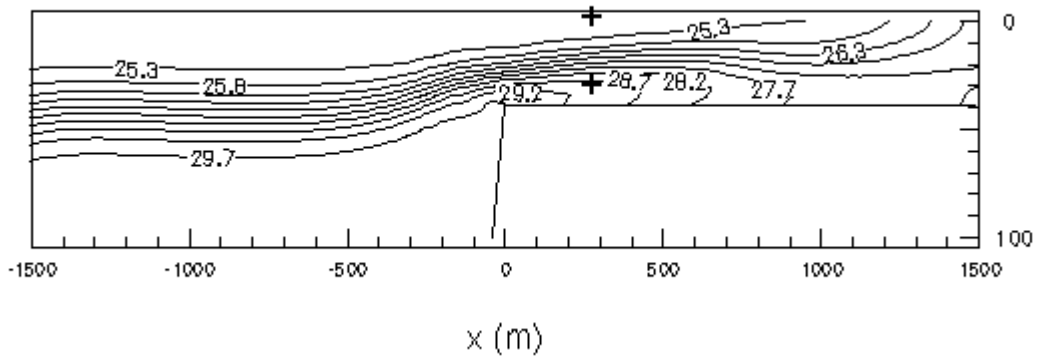
Here, we present some results of a numerical experiment with an  $80^\circ$  angle of the shelf plateau declination. In Fig.1, vertical sections of the salinity field are drawn. They correspond to 0.5 and 0.95 moments of the M2 period (T). These situations are marked in Fig. 2, where salinity and kinetic energy timeserias at two different levels obtained in the numerical experiment are presented. On the contrary, in Fig.1 are marked the points where these timeserias were obtained.

Both figures illustrate a very asymmetrical picture of the deep water expansion toward the plateau in time. Its maximum coincides with the last part of the M2 period (see Fig. 1). In Fig. 2a, near the surface, after an abrupt decrease of the salinity in the middle of the M2 period, the salinity monotonically arises during all of the other part of the period. A more complex situation exists in the middle of the above plateau volume. Here, after an abrupt decrease in salinity, nearly the same abrupt increase of it follows. For the most part of the M2 period the salinity irregularly oscillates slightly above its mean value for this level. In Fig. 2b, after abrupt increase of the kinetic energy in the middle of the period its fluent decrease follows.

An additional point is to emphasize that in numerical experiments with a coarse resolution nest grid (about 50 m) the complex feature of this curve diminishes and, what is especially important, the situation on the right-hand outflows is different.

For a more precise investigation of the process of the internal wave breaking, which coincides with abrupt changes of the salinity during the M2 period, spectral analysis of the timeserias of salinity, kinetic energy, turbulent kinetic energy and its dissipation rate are fulfilled.

a)



b)

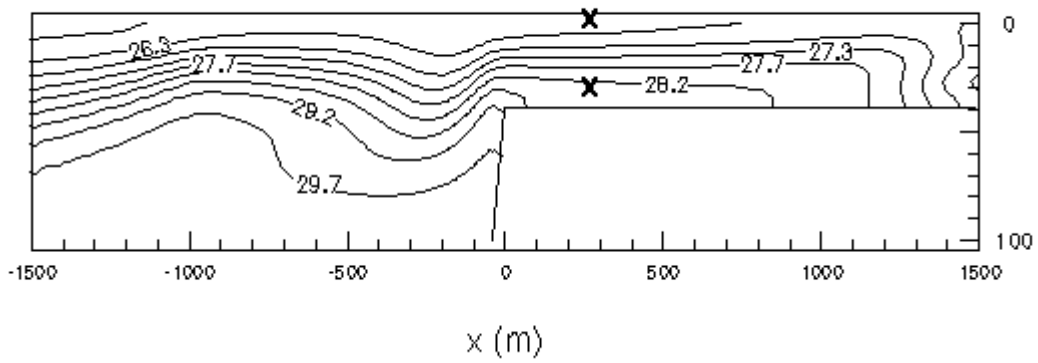


Figure 1. Vertical section of the salinity field: (a) 0.5 T; (b) 0.95 T.

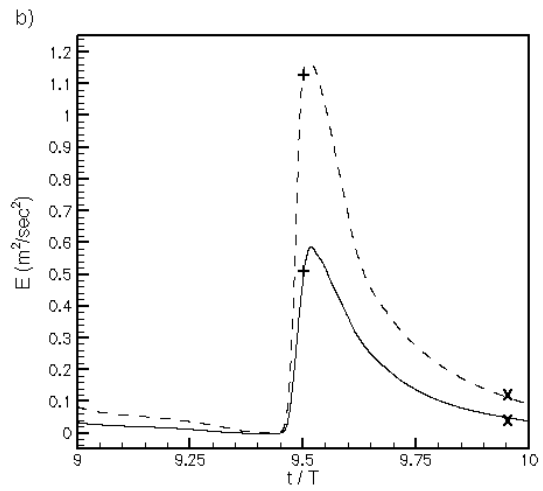
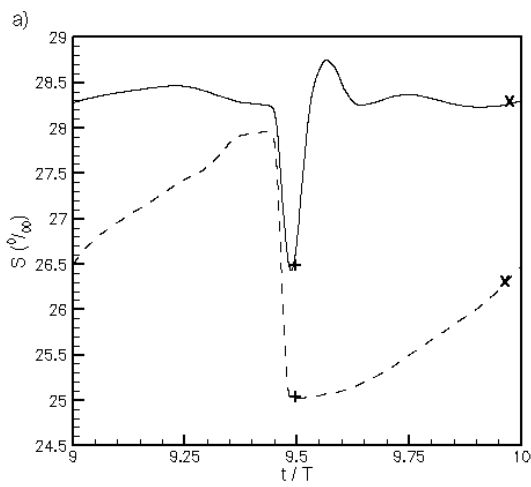


Figure 2. Time series of salinity (a) and kinetic energy (b).  
 — 26.9 m, - - - 3.84 m; + - 0.5 T, x - 0.95 T.

# Development of a Coupled Ice-Ocean Model of Hudson Bay

S. Senneville<sup>1</sup>, F. J. Saucier<sup>1</sup>, P. Gachon<sup>1</sup>, R. Laprise<sup>2</sup> and D. Caya<sup>2</sup>

<sup>1</sup>Ocean Sciences Branch, Department of Fisheries and Oceans, Mont-Joli (Qc) Canada

<sup>2</sup>Dept. Earth and Atm. Sciences, Université du Québec à Montréal, Montreal (Qc) Canada

e-mail: sennevilles@dfo-mpo.gc.ca

The seasonal cycle of water masses and sea ice production and circulation in the Hudson Bay basin is examined using a baroclinic coastal ice-ocean model including a level 2.5 turbulent kinetic energy equation. The resolution of this model is 10 km in the horizontal and 10 to 50 m in the vertical. The time step is 5 minutes. The domain includes Foxe Basin, Hudson Strait, and James Bay. The model is driven from tidal, atmospheric, hydrologic and oceanic forcing, as done for the Gulf of St. Lawrence in Saucier et al. (2002). The aim is to first reproduce the main features (e.g., transports, heat, freshwater and sea-ice seasonal cycles) using 3-hourly atmospheric reanalyses, and then to couple this model into the Canadian Regional Climate Model (CRCM) (Caya and Laprise, 1999) and into the Global Environmental Multiscale (GEM) model (Côté et al., 1997) for improving and downscaling climate change scenarios and the Canadian operational weather forecast, respectively.

A model simulation over 1996-97, driven by the CMC Regional Finite Element (RFE) and GEM reanalyses, is verified against climatological data. The model is forced at the mouth of Hudson Strait from 10 harmonic components obtained from Matsumoto et al. (2000). Figure 1 shows the modelled co-phase and co-amplitude chart for the M2 tidal harmonic. The mean relative error in amplitude is 9% and the RMS phase error is 20° for 9 tide gauge shore stations around the domain. The mean surface currents (Figure 2) reproduce the general pattern reported from observations. Freshwater from major tributaries around the Bay form a coastal current exiting through Hudson Strait and partly re-circulating through the Bay. The sea-ice cover growth during fall 1996 is presented in Figure 3 with the evolution of the 5 cm ice thickness contour at 10 day intervals over the period extending between November 18 and December 28. The presence of higher values for thickness and concentration of sea-ice in the southern part of Hudson Bay near the end of the simulation in July is also well reproduced by the model (not shown). Figure 4 shows the domain-averaged salinity, temperature, and turbulent kinetic energy (TKE) over the simulation period. The salinity shows the effect of salt rejection associated with sea-ice growth, followed by a reduction associated with the late spring runoff. The temperature shows the deepening of the surface mixed-layer in fall, with wind-driven mixing reaching about 100 m depth. Finally the seasonal cycle of TKE shows a strong neap to spring tidal cycle near the bottom of Hudson Bay, and little wind-induced TKE under sea-ice. These results show a consistent seasonal cycle in atmosphere-ocean exchanges, mixing, and the formation and circulation of water masses and sea ice.

The modelled delay in freeze-up dates in the fall is related to the accuracy of the low-level atmospheric fields (e.g., lower winds and higher temperature) which leads to relatively large biases in the mixed-layer heat cycle and sea ice production. These results point to the importance of improving the atmospheric model as it is the foremost limiting factor in the accuracy of ocean solutions. Once a balanced seasonal cycle is obtained, the model can be run over a period of several years to a decade in order to examine climate variability and changes associated with the atmospheric and hydrological forcing.

## References:

- Caya D., and R. Laprise. A semi-implicit semi-lagrangian regional climate model: The Canadian RCM. *Mon. Wea. Rev.*, 127, p. 341-362, 1999
- Côté J., S. Gravel, A. Méthot, A. Patoine, M. Roch, and A. Staniforth. The operational CMC/MRB Global Environmental Multiscale (GEM) model: Part I – Design consideration and formulation, *Mon. Weather Rev.*, 126, 1373-1395, 1997
- Matsumoto K., T. Takanezawa, and M. Ooe, Ocean Tide Models Developed by Assimilating TOPEX/POSEIDON Altimeter Data into Hydrodynamical Model: A Global Model and a Regional Model Around Japan, *Journal of Oceanography*, 56, 567-581, 2000.
- Saucier F. J., F. Roy, D. Gilbert, P. Pellerin, and H. Ritchie (accepted). Modelling the formation and circulation processes of water masses and sea ice in the Gulf of St. Lawrence, Canada. *J. Geophys. Res.*

**Results :**

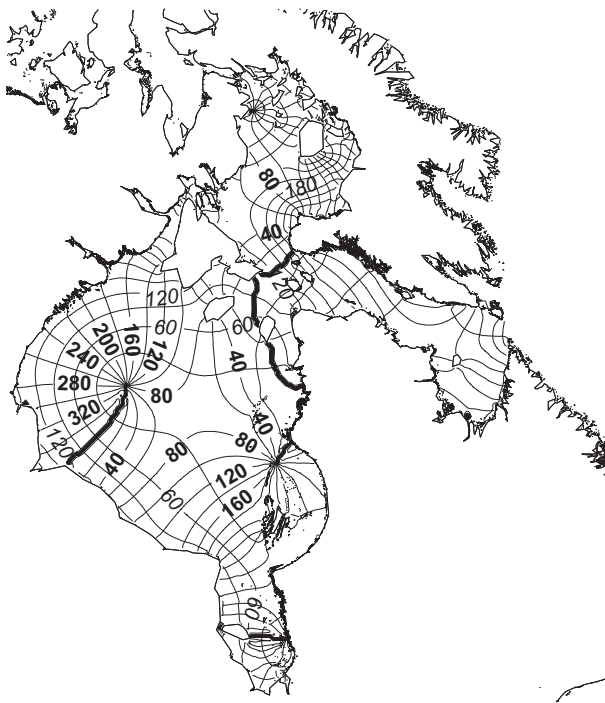


**Figure 1: Tidal chart of M2 component : Co-amplitude (bold) and co-phase (italic).**

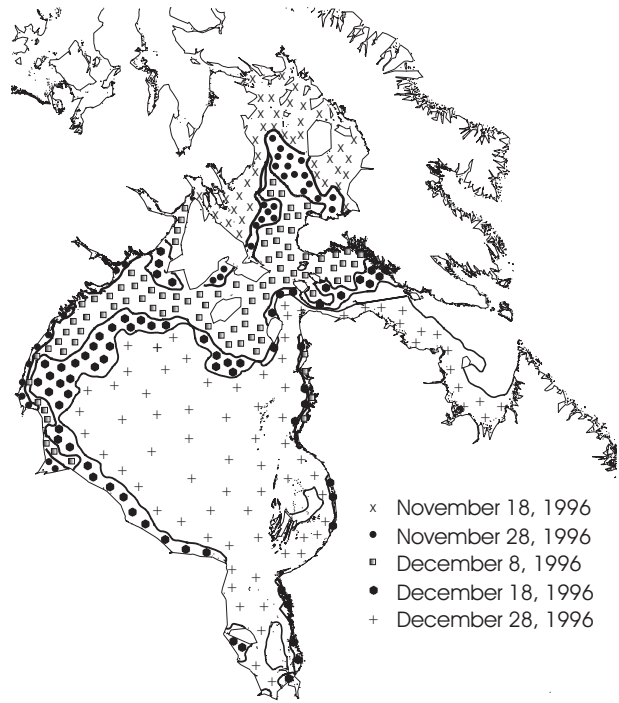


**Figure 3: Date of sea-ice formation over 5cm thickness**

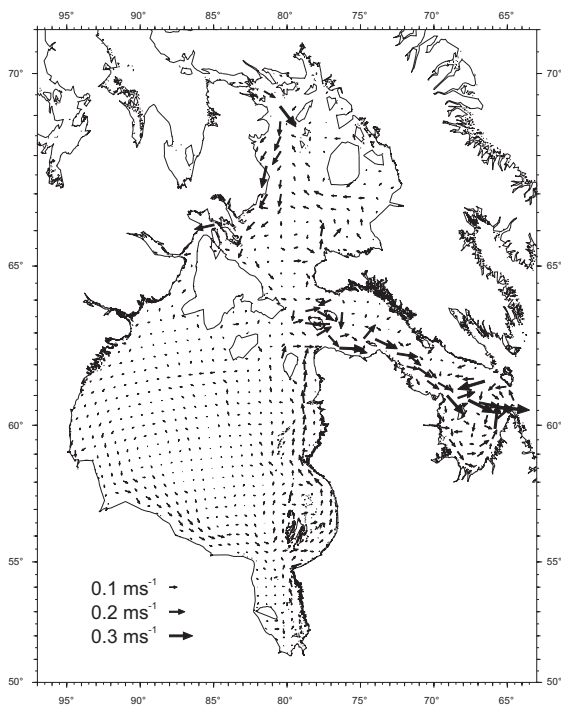


**Figure 2: Yearly mean surface current (surface 10m)**

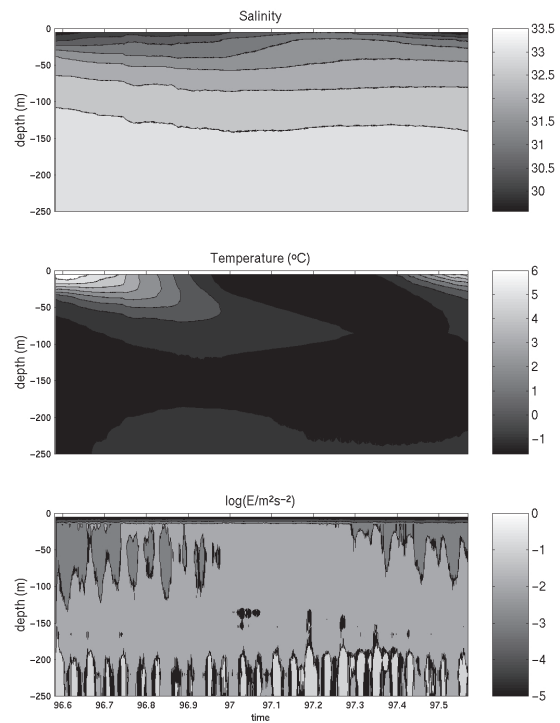


**Figure 4: Domain-averaged salinity, temperature, and turbulent kinetic energy**

Hydrodynamic modeling the coastal surface currents  
for the water pollution problems.

Shnaydman V.A.

Department of Environmental Sciences, Rutgers University-Cook college  
14 College Farm Road, New Brunswick, NJ, 08901 USA

e-mail: [Volf@envsci.rutgers.edu](mailto:Volf@envsci.rutgers.edu)

Tarnopolskiy A.G.

Department of Geophysical Hydrodynamics, Ecological University,  
Lvovskaya 15, Odessa, Ukraine,

e-mail: [geophys@ogmi.farlep.Odessa.ua](mailto:geophys@ogmi.farlep.Odessa.ua)

A three-dimensional, time-dependant, baroclinic model for the coupled atmospheric and coastal shelf boundary layers (thereafter ABL and SBL, correspondingly) is applied to study polluted effluents (mostly oil residues) transport (1,2). One such application stands alone for it is essentially a study of the backward chronology of a pollution event.

The coupled ABL and SBL model was used to reconstruct the current and property fields for the entire pollution episode with known external forcing factors. Since the pollutant was positively buoyant, only surface currents were of interest, although the model provided the multilayered picture.

The coupled ABL and SBL model allows implementation of a two-step procedure to obtain the surface currents. At the first step the ABL model with given pressure field is transformed to use the actual surface winds instead of the geostrophical ones. This transformation is needed to solve the backtracking of the source on the basis of information of the actual winds. Then the ABL modeling is used to determine the turbulent flux of momentum through the water surface. At the second step the Reynolds stresses obtained were used in the SBL modeling for quantitative description of the atmospheric dynamical forcing. The atmospheric motions form the turbulent flux of momentum which goes into formation of the drift currents and the deviation of the free surface from equilibrium value due to the wind impact, breaking the surface waves. The SBL modeling takes into account the parts of the atmospheric turbulent momentum fluxes that form separately currents and wind waves, the creation of pure "wind drift" that then goes into formation of what is perceived as the geostrophical currents, the flux of kinetic turbulent energy due to waves collapse.

The important SBL hydrodynamics mechanism is the vertical turbulent exchange which is described by the two-equation scheme (turbulent kinetic energy and dissipation rate).

The comparison with observations in the study area shows a good agreement between simulated and measured surface currents velocities.

We show an example of application the two-step procedure to backtrack the source of the oil plume which allowed the authorities to correct the wrong conclusion of the source location. The plume was detected at noon (May 9,1996) near the Odessa South Seaport. The well-defined plume moved from east to west what allowed to conclude that the plume was released by the tanker located in the eastern side of South Seaport. But the chemical test didn't confirm this conclusion. The detail analysis of the meteorological information showed that the wind directions were changed during the period between 12:00 May 8 and 12:00 May 9. This information is given in the table where  $V_s$  is the module,  $D_s$  is the direction of the wind over the land and sea properly,  $V_c$  and  $D_c$  are the module and the direction of the surface current vectors. The backward trajectory is computed on the basis of calculated currents allowing detection of the polluted plume. This trajectory is directed from west to east from 12:00 ET to 22:00 ET May 9, from east to west from 22:00 ET May 9 to 10:00 ET May 8 and then before 10:00 ET May 8 turned to east. The trajectory's behavior clearly indicated that the source is located near the point of the trajectory at 10:00 ET May 8. where the distance between the plume and the coast was the smallest. Actually the source of the oil slick turned out to be the power station located on the coastal area.

t, ET	12	15	18	21	00	03	06	09	12
<b>Land</b>									
<b><math>V_s</math>, m/s</b>	<b>3</b>	<b>4</b>	<b>4</b>	<b>2</b>	<b>3</b>	<b>2</b>	<b>2</b>	<b>2</b>	<b>2</b>
<b><math>D_s</math>, deg.</b>	<b>3 45</b>	<b>3 45</b>	<b>45</b>	<b>45</b>	<b>270</b>	<b>270</b>	<b>225</b>	<b>180</b>	<b>90</b>
<b>Sea</b>									
<b><math>V_s</math>, m/s</b>	<b>5,4</b>	<b>7,2</b>	<b>7,2</b>	<b>3,6</b>	<b>5,4</b>	<b>3,6</b>	<b>3,6</b>	<b>3,6</b>	<b>3,6</b>
<b><math>D_s</math>, deg.</b>	<b>30</b>	<b>30</b>	<b>30</b>	<b>30</b>	<b>255</b>	<b>255</b>	<b>210</b>	<b>165</b>	<b>75</b>
<b>Sea</b>									
<b><math>V_c</math>, cm/s</b>	<b>7,6</b>	<b>14,5</b>	<b>14,5</b>	<b>4,0</b>	<b>9,8</b>	<b>7,0</b>	<b>6,0</b>	<b>5,7</b>	<b>3,8</b>
<b><math>D_c</math>, deg.</b>	<b>346</b>	<b>348</b>	<b>354</b>	<b>355</b>	<b>210</b>	<b>220</b>	<b>190</b>	<b>150</b>	<b>45</b>

1. Berkovich, L.V., Tarnopolskiy, A.G., Shnaydman, V.A.: 1997, 'A Hydrodynamic Model of the Atmospheric and Oceanic Boundary Layers', Russian Meteorology and Hydrology 7, 22-31

2. Shnaydman, V.A., Tarnopolskiy, A.G.: 1999, "Conception of the Investigation of Anthropogenic Forcing on the Sea Environment", Dokl. NAS of Ukraine 2,204-208.

# Oceanic State During 1993-1999 Determined by 4-D VAR Data Assimilation

J. Staneva, M. Wenzel and J. Schröter

Alfred Wegener Institute for Polar and Marine Research

Bussestr. 24, D-27570 Bremerhaven, Germany e-mail: jstaneva@awi-bremerhaven.de

We study here the variability of sea level and oceanic state during 1993 - 1999 using 4D VAR data assimilation. The ocean data assimilation is directed to the combined use of ocean and data to obtain a time dependent oceanic state. The recent progress in understanding the ocean circulation depends upon the availability of ocean observations. Hydrography data however are sparse in space and time. TOPEX/POSEIDON satellite altimetry measures the sea level variability at global scales every 10 days with an accuracy of the anomaly less than 5 cm (Cheney et al., 1994). The variability of the sea surface height gives an integral measure of the three-dimensional ocean circulation. Here we use the Hamburg LSG model to study the state of the ocean. It is a coarse resolution OGCM ( $3.5^\circ \times 3.5^\circ$  horizontal and 11 vertical levels) originally designed for climate studies. The implicit formulation in time of the LSG allows for a time step of one month. To combine the model and data we use the adjoint method. As control parameters we use the model initial temperature and salinity state and the mean annual cycle of wind stress, air temperature and freshwater flux. The additional temporal variability of the forcing is taken from the NCEP reanalyses from 1992 to 1999. Additionally we utilise the same data sets as in Wenzel et al. (2001), but with reduced weights. The initial state is taken from its optimised climatological annual cycle obtained by Wenzel et al. (2001). As a reference for our purpose the LSG model is forced subsequently with monthly data from the NCEP reanalysis project for 1950-1999. The first guess initial model state and forcing fields are taken from the oceanic state in January 1992. Seven years (1993-1999) of TOPEX/POSEIDON (T/P) sea surface height relative to the EGM96 geoid model are also assimilated into the model.

First we compare the variability of the simulated sea surface height from the model with the variability of T/P data (figure 1). The horizontal patterns of the variability of the Sea Surface Anomaly (SSA) of T/P altimetry data is quite similar to that obtained by the constrained model. The largest differences between the variability of the altimetry data and model simulations are observed in the equatorial Pacific and Indian oceans. The deviations of the SSA variability obtained by the constrained model from that of the T/P anomalies are better pronounced in the regions of the strong currents.

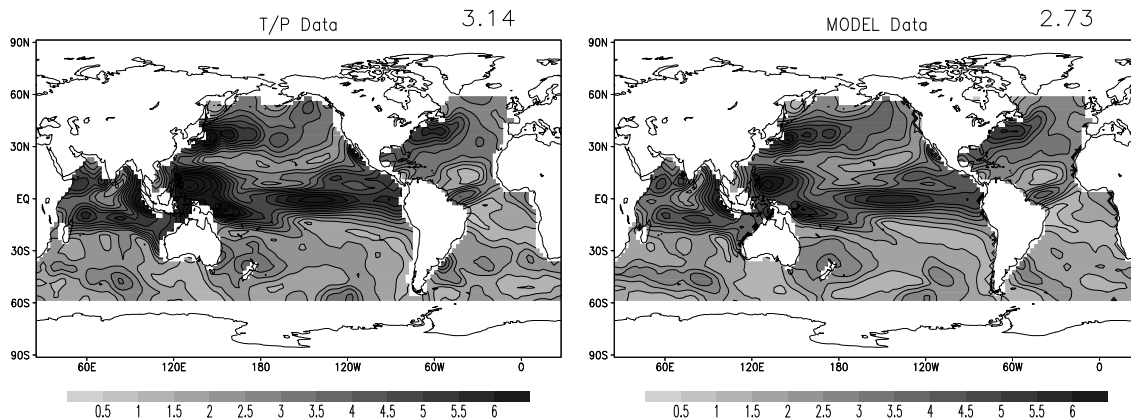


Figure 1: RMS variability of sea surface height [cm] from the T/P data (left) and optimised model (right) averaged from 1993 to 1999.

The area mean variability of SSA (see figure 2) in constrained solution (dashed line) from 1993 to 1999 is closer to that of the T/P data (full line). Some deviations of the model solutions from the T/P data are observed at the end of integration period.

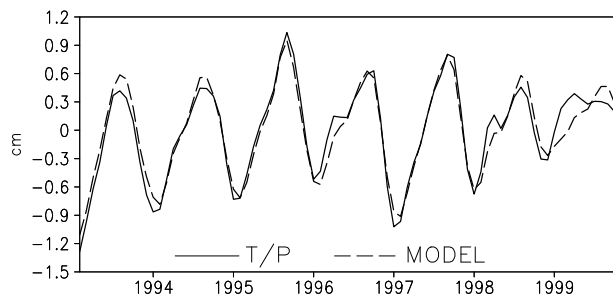


Figure 2: Area mean sea surface anomaly [cm] as a function of time (c): full line-T/P data, dashed line - optimised model data.

The temperature and salinity of the model are constrained using Levitus monthly mean climatological fields (Levitus, 1994). Below we will compare the model simulations with this climatology as well as with independent data set taken from WOCE hydrography. The differences between the temperature estimated by the constrained model and the temperature taken from the Levitus climatology and WOCE data are shown in figure 3 across the central Pacific depth-longitude section ( $32.5^{\circ}\text{S}$ ). The temperature from the model simulations and climatological data is time averaged from May to July. The WOCE hydrology and Levitus data are interpolated to the model grid, therefore all small scale structures related to the eddies in the WOCE hydrography are eliminated. The large-scale structures simulated by the model are with visually good agreement with the the data. The temperature differences are mainly pronounced in the upper 1000 m. The sub-surface temperature obtained by the constrained model exceeds that of the data, indicating the model deficits due to its coarse horizontal resolution. It is clearly seen from the vertical sections that the temperature of the assimilation experiment compares better to the independent temperature of the WOCE section than to the Levitus climatology, indicating that the model stratification tends to be closer to the real hydrological data rather than to climatological one. Giving most weight to the constraints on sea surface height improves the density of the model to a structure more realistic than climatology.

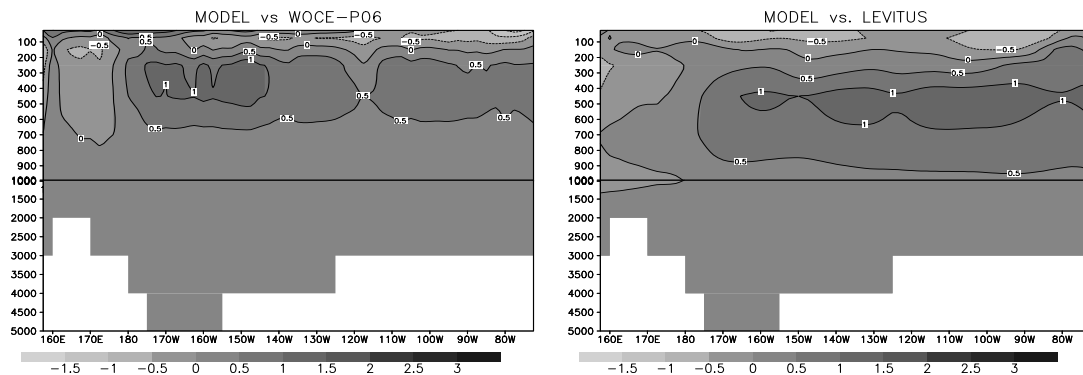


Figure 3: A comparison of depth-longitude section of temperature ( $^{\circ}\text{C}$ ) taken at  $32.5^{\circ}\text{E}$  across Pacific and time averaged between May and July for: (left) model simulations *vs.* WOCE data. and (right) model simulations *vs.* Levitus data

*Acknowledgements: This work was supported by HGF Strategiefonds-Project 2000/13 SEAL Project.*

### References:

- Levitus, S., R. Burgett and T. Boyer, 1994: World Ocean Atlas 1994, vol. 3, Salinity and vol. 4, Temperature, NOAA Atlas NESDIS 3 and 4, U.S. Dept. of Comm., Washington, D.C.
- Cheney, R., L. Miller, R. Agreen, N. Doyle and J. Lillibrige, 1994: TOPEX/POSEIDON: 2 cm solution. *J. Geoph. Res.*, 99, 24555-24563.
- Wenzel, M, J. Schröter and D. Olbers, 2001: The annual cycle of the global ocean circulation as determined by 4D VAR data assimilation. *Progr. in Oceanogr.*, 48, 73-119.

# IMPROVEMENT OF SST PREDICTION BY DIUNAL CYCLING ALGORITHM IN THE MRI MIXED LAYER OCEAN MODEL

Akiyoshi Wada

Meteorological Research Institute, Tsukuba, Ibaraki, Japan  
awada@mri-jma.go.jp

## 1. Introduction

Recently, many researchers have recognized the importance of the sea surface temperature (SST) particularly local SST cooling for intensities of tropical cyclones (TCs), and have studied the relationship between the SST and the intensities of TCs by various methods. It is necessary to estimate the SST more accurate in order to improve forecasts of intensities of TCs. A SST is usually determined by sea surface heat fluxes, horizontal and vertical advection, and entrainment process and so on. With regard to sea surface heat fluxes, solar insolation is considered to be the most important among surface heat fluxes to determine the SST because solar heating warms and stabilizes the upper ocean at midday. However, the contribution of sea surface heat fluxes for the SST variation will be underestimated in a mixed layer ocean model owing to its deep mixed layer if we simply formulate the net heat flux as the sum of sensible, latent, long-wave and short-wave radiative heat fluxes. Solar insolation is absorbed in the water column at most 0 (10m), while the heat loss calculated by sensible, latent, and long-wave radiative heat fluxes is presumed to leave directly from only sea surface. Here, the algorithm of Price et al. (1986) (diurnal cycling algorithm) is partly applied within the mixed layer in the Meteorological Research Institute (MRI) mixed layer ocean model. We state the detail of this MRI mixed layer ocean model (updated MRI mixed layer ocean model), and then we indicate the model performance for maritime observation data obtained by Keifu-Maru, which is the research vessel and belongs to Japan Meteorological Agency, through the cruise on August 1998. After some inspections including this paper, we will plan to apply this model to Typhoon-ocean coupled model.

## 2 Numerical models

The construction of the MRI mixed layer ocean model is referred to Wada (2002). Beyond this, we include the processes of horizontal viscosity for ocean currents and diurnal cycling algorithm in the MRI mixed layer ocean model. As for the diurnal cycling algorithm, we set to 1m as the vertical grid resolution within the mixed layer (30m). At a top layer, a SST is affected by net heat flux (sensible, latent, and long-wave radiative heat fluxes) and solar insolation. Absorption or transmission rates of solar insolation depend on the depth and are estimated by formulas of Price et al. (1986). Except the top layer, only solar insolation affects the SST within the mixed layer at midday. If the density inversion occurs at each layer within the mixed layer, the layer is stirred and stabilized. At last, the SST in the updated MRI mixed layer ocean model is determined as an average of second and third layer (equivalent to 2.5m depth). After this diurnal cycling algorithm is completed, the advection term and the entrainment term in thermodynamics equations are estimated. Absorption rates at the top layer are also used to estimate the part of natural convection by entrainment.

## 3. The numerical experiment in case of the field observation

We conducted a numerical experiment in order to inspect the performance of the diurnal cycling algorithm. The CTD data acquired by Keifu-Maru on August 23 around 130° E, 20° N were used to determine the oceanic vertical profiles of sea temperature and salinity, which are assumed to be horizontally constant, however the SST was determined by maritime data. We also used maritime data (air temperatures and winds) by Keifu-Maru as the atmospheric initial and boundary conditions from August 23, 1998 to August 26, 1998. Maritime data by Keifu-Maru were obtained every 10 minutes except the total cloud cover in tenths by visual observation in every three hours. The time step of the MRI mixed layer ocean model was set to 20 minutes so that atmospheric boundary conditions changed in every time step. The long-wave radiative flux and solar insolation were respectively determined by bulk formulas included the total cloud cover. According to Figure 1, the SST variation in the updated MRI mixed layer ocean model is similar to that of the SST observed by Keifu-Maru. During the periods of the experiment, diurnal cycling appeared from August 25, 1998 to August 26, 1998 and this period agreed with the time when the total cloud cover was less. In addition, the decreasing slope of predicted SST in the updated MRI mixed layer ocean model was suitable for that of observed SST during the nighttime particularly when the wind speed was over 10m/s.

4. The numerical experiment in case of moving typhoon (Typhoon Rex in 1998).

We inspected the model performance by applying the case of Typhoon Rex shown by Wada (2002). Wada (2002) realized a local 3°C cooling of SST by passage of Typhoon Rex using the MRI mixed layer ocean model, however SST cooling tended to be underestimated with the model. The underestimation of SST cooling seemed to be caused by errors of bulk coefficients. In this report, the SST cooling by passage of Typhoon Rex is better expressed with the updated mixed layer ocean model (Figure 2). The prominent results shown in Figure 2 are the following:

1) A gentle decrease of SST is well simulated from August 24, 1998 to August 27, 1998.

2) The amount of the maximum SST cooling is well simulated under the same modification of bulk coefficients as introduced to Wada (2002).

It is convinced that the variance of SST is better simulated by diurnal cycling algorithm, however model-computed SST seems to be lower than SST observed by Keifu-Maru at a region of the Kuroshio after August 29, 1998, which is one of the future problem in developing the mixed layer ocean model.

References

Price, J. F., and Weller, R. A. 1986: Diurnal Cycling: Observations and models of the upper ocean response to diurnal heating, cooling, and wind mixing. *J. Geophys. Res.*, 91, 8411-8427.

Wada, A 2002: The processes of SST cooling by typhoon passage and case study of Typhoon Rex. *Pap. Meteor. Geophys.* Accepted

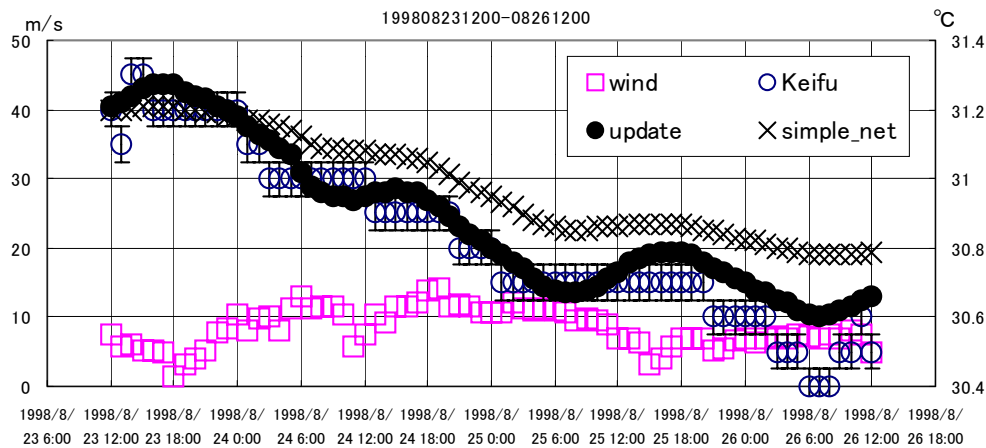


Figure 1 Time series of the observational SST by R/V Keifu-Marui, the SST by simply surface net flux, and the SST by updated mixed layer ocean model from August 23, 1998 to August 26, 1998.

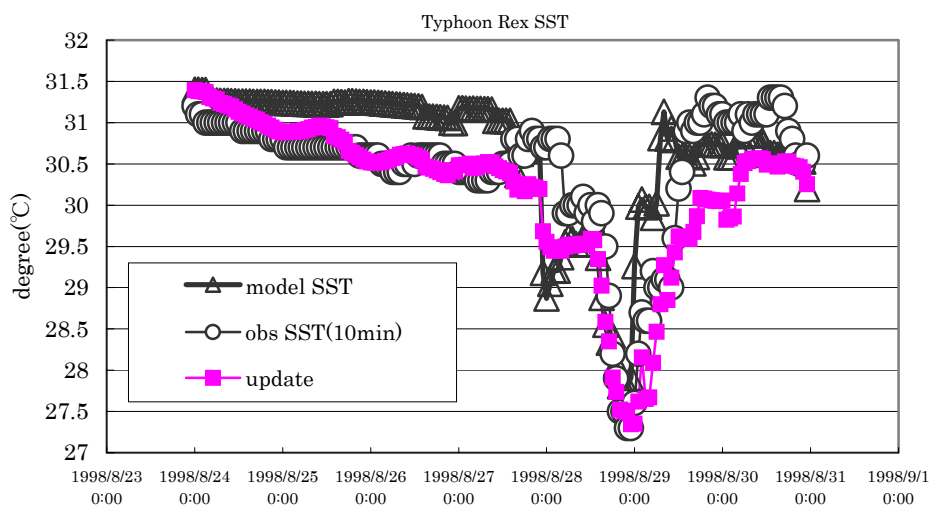


Figure 2 Time series of the observational SST by R/V Keifu-Marui, the SST by Wada (2002), and the SST by updated mixed layer ocean model. from August 24, 1998 to August 31, 1998.

# A Numerical Study of the Circulation on the Western Shelf of the Gulf of Mexico

Jorge Zavala-Hidalgo, Steven L. Morey, and James J. O'Brien  
Center for Ocean-Atmospheric Prediction Studies, The Florida State University

The seasonal to synoptic scale circulation on the western shelf of the Gulf of Mexico (WSGM) is studied using the Navy Coastal Ocean Model (NCOM) (Martin, 2000; Morey *et al.*, 2001). The model domain includes the entire Gulf, from 15.55°N to 31.50°N and from 80.60°W to 98.15°W, in a 1/20° resolution C grid with 20 sigma coordinates in the upper 100 m and 20 z-level coordinates below 100 m. The domain includes the entire Gulf because of the importance of the remotely generated Loop Current eddies on the western Gulf. The model is forced with monthly mean fluxes at the surface, a prescribed constant current in the open boundary at the Caribbean Sea, and an open boundary at the Florida Strait.

The WSGM is characterized by a wide shelf off the coast of Louisiana and Texas (LATEX) of around 200 km that narrows toward the south in the Mexican states of Tamaulipas and Veracruz, becoming narrowest (~40 km) in the southern part of the Campeche Bay (Fig. 1). There are not many previous studies in this region (Boucourt *et al.*, 1998) so we focus this study on the dynamics at a seasonal scale.

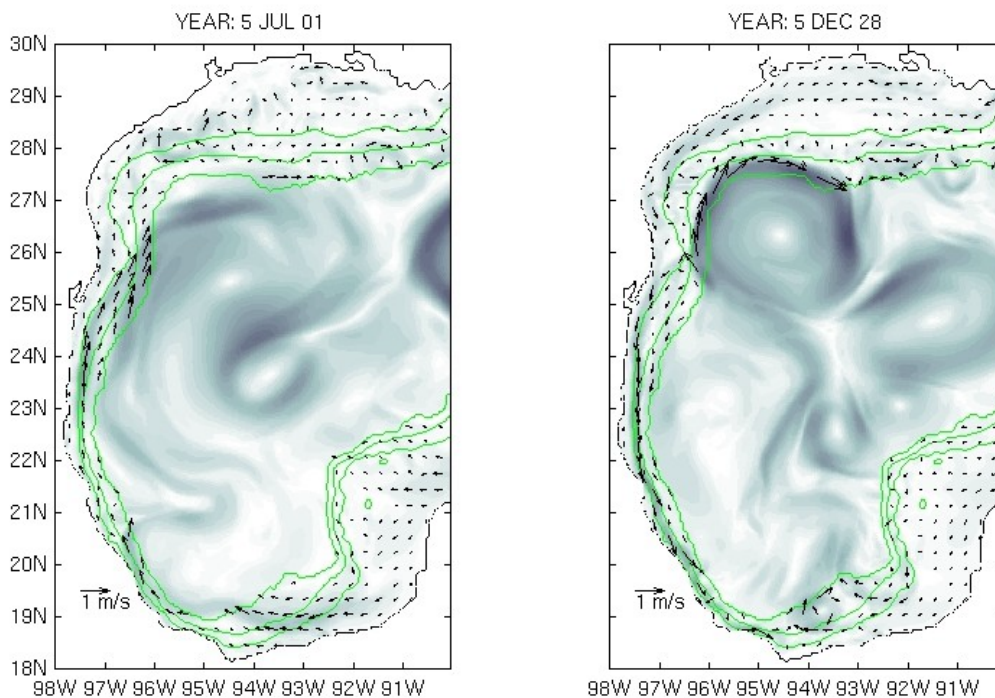


**Figure 1.** Surface velocity on the shelf of the western Gulf of Mexico for representative days of the spring-summer (July 1) and fall-winter (December 28) conditions. Also contours of the 50, 200, and 1000 m depth.

Our results show that there is a strong seasonal component in the circulation variability of the WSGM. During spring-summer, south of 27°N, the dominant circulation is to the north, beginning in March-April. The summer regime remains until early September when the circulation reverses to a counterclockwise direction (Fig. 1). Velocities are typically ~50 cm/s, and transports between the coast and the 50 m isobath vary from 0.1 to 0.5 Sv. Most of the seasonal signal is confined between the coast and the location of the 50 m isobath, but this varies in different locations of the shelf. South of 26°N, where the continental shelf is narrower, the seasonal signal reaches as far as the 200 m isobath. The fall-winter current reaches the southern Bay of Campeche where it collides with an along-shelf current running in the opposite direction.

During winter, fresh water from the Mississippi and Atchafalaya rivers is advected along the LATEX shelf onto the Tamaulipas shelf, developing along-shelf thermal and salinity fronts (Fig. 2). The summer

circulation is associated with an upwelling generated by local Ekman transports with sloping isotherms and a northward along-shelf current (Fig. 2).

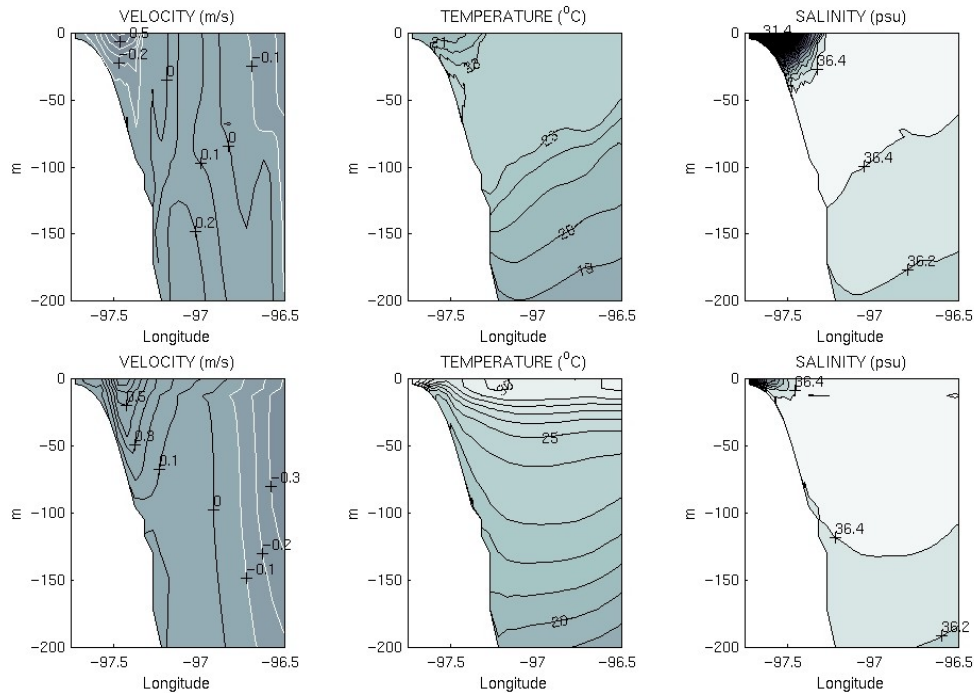


**Figure 2.** Vertical sections of meridional velocity, temperature, and salinity at 24°N for representative days of spring-summer (upper panel) and fall-winter (lower panel) conditions.

The seasonal circulation is caused by the combination of the local wind stress forcing and an important remote component caused by coastal waves originating in the LATEX shelf as follows. During winter the Ekman transport on the LATEX shelf piles water toward the coast developing coastal Kelvin waves that migrate southward. Associated with these waves is a coastally attached current running counterclockwise that continues along the Mexican shelf. The current is trapped by the topography and reinforced by the local Ekman transport. From April to September the Ekman transport in the LATEX shelf shifts 90 degrees clockwise generating an eastward transport along the external shelf. Over the Mexican shelf, the local winds in the Mexican shelf change direction favoring upwelling.

### Acknowledgments

Special thanks to Paul Martin and Alan Wallcraft from the Naval Research Laboratory for their support in the implementation of the NCOM simulation of the Gulf of Mexico. The simulation was performed on the IBM SPs at the Florida State University and the Naval Oceanographic Office with computer time provided by the High Performance Computing Modernization Office. The project was sponsored by funding provided by the DoD Distributed Marine Environment Forecast System and by the Office of Naval Research Secretary of the Navy grant awarded to Dr. James J. O'Brien.

### References

Boicourt W. C., W. J. Wiseman Jr., A. Valle-Levinson, and L. P. Atkinson, 1998: Continental Shelf of the Southeastern United States and the Gulf of Mexico: In the shadow of the Western Boundary Current. *The Sea*, Vol 11, Allan Robinson and Kenneth H. Brink Eds., 135-182.

Martin P. J., 2000: A Description of the Navy Coastal Model (NCOM) Version 1.0. Naval Research Laboratory, NRL/FR/7322-00-9962, 42 pp. Washington, D. C.

Ocean Modeling of the Gulf of Mexico. Research Activities in Atmospheric and Ocean Modeling, CAS/JSC Working Group on Numerical Experimentation, 2001.